INTEGRATED THERMOCHEMICAL CONVERSION PROCESSES FOR THE PRODUCTION OF SOIL AMENDMENTS AND BIOFUELS FROM AGRICULTURAL WASTE

A Thesis

Presented to the Faculty of the Graduate School

of Cornell University

In Partial Fulfillment of the Requirements for the Degree of

Master of Science

by

Jui-Chun Lin

May2020

ABSTRACT

The demand for food and energy resources is continuously increasing as the global population grows. Conventional fertilizers are used to promote crop growth to meet these demands, but also lead to adverse environmental issues such as nutrient runoff. Biochar is a promising soil amendment alternative that is produced from hydrothermal carbonization (HTC) or pyrolysis technologies. However, neither process is ideal - HTC is suitable for wet biomasses, but the produced hydrochars suffer from low surface area; Pyrolysis is suitable for dry biomasses, but the produced biochars contain low nutrient content. We proposed an integrated HTC/pyrolysis process to produce biochars by co-pyrolyzing cow manure hydrochar with raw agricultural residues. The physical characteristics (i.e. proximate analysis, pH, surface area, nutrients…etc.) and heating value of char products were investigated for use as solid fuels. The integrated HTC/pyrolysis process demonstrated an enhancement in bioavailable nutrients, but the surface area is sample dependent. Results revealed that the biochars are ideal for soil amendment, while the hydrochars are generally more suitable for solid fuel applications.

BIOGRAPHICAL SKETCH

Jui-Chun Lin is an M.S. candidate in the Biological and Environmental Engineering department at Cornell University. He received his B.S. in Energy Engineering from The Pennsylvania State University. At Penn State University, he was an undergraduate research assistant on a stainless-steel corrosion project and have worked on several lab equipment. His current focus at Cornell University is on the combination of two thermochemical processes for renewable bioproducts improvements.

ACKNOWLEDGMENTS

I would like to express my sincere appreciation to the people who gave me feedback and guidance over the past two years during my Master of Science journey. I am particularly thankful for my principal investigator, Dr. Jillian L. Goldfarb, who is not only my advisor, my teacher, but also a life mentor who encouraged me to be professional and do the right thing even in tough situations. Without her persistent help, finishing this degree would be nearly impossible. I am also grateful for my graduate committee (Dr. Jefferson W. Tester and Dr. Luca Fiori) that have been giving me feedback and critiques on my research work. Thank you Dr. Jefferson W. Tester and Dr. Kui Wang for letting me use your elemental analyzer. In addition, I would like to thank my fellow peers (Dr. Fei Wang, Liyang Ma, Qiulin Ma, Andrew Hubble, Zoe Pollard, Matteo Pecchi, Madeline Karod, Dylan Mariuzza) for the constant supports and discussions, making the lab space and the office space fun places to be around. I would like to pay my special regards to Dr. Alex Maag. Thank you for constantly helping me with data interpretation and troubleshooting the equipment. Lastly, I am extremely grateful to my family, who have always been supported and encouraged me throughout my time at Cornell University.

TABLE OF CONTENTS

Chapter 1: Introduction

Food, water, and energy demands are some of the most significant challenges humanity are presently facing in a world of rising population. The agricultural industry consumes the vast majority of the water, nutrient, and land resources. The overuse of chemical fertilizers to increase crop yield also pollutes the water and land from runoffs. Moreover, the dairy industry across the globe contributes significantly to global greenhouse gas emissions, accelerating global warming. A commonly assumed management strategy for animal waste, such as manure, is direct land spreading, owing to their relatively high nutrient contents as fertilizers.[1] However, the unprocessed waste is prone to decompose under ambient conditions, releasing greenhouse gases into the atmosphere. In fact, the direct spreading of farm waste represents a potential waste of valuable carbon, but it also causes the unbalancing of soil dynamics.[2,3] By converting farm and animal waste to nutrient-enriched soil amendments and biofuels via integrated thermochemical conversion processes, it is possible to achieve several goals: (1) lower resource consumption; (2) enhance nutrient use efficiency; (3) increase crop yields without the use of conventional fertilizers; (4) improve renewable energy deployment and (5) lessen anthropogenic environmental impacts of industrial agriculture. Two main thermochemical processes are promising approaches to convert biomass into more valuable products: Hydrothermal carbonization (HTC), which the sample is heated under subcritical conditions in water, and pyrolysis, which the sample is heated under an inert atmosphere.

While both HTC and pyrolysis convert carbonaceous waste to hydrochars and biochars, respectively, neither alone is a perfect solution to waste management. HTC allows converting using wet biomasses directly with concentrated P and N inside the solid hydrochar; pyrolysis can treat dry biomasses producing materials with high surface areas. Past literature has demonstrated that hydrothermal carbonization is suitable to treat wet biomasses such as municipal solid waste and cow manure to concentrate nutrients in a solid amorphous carbon.[4] HTC has the ability to concentrate and immobilize nutrients present in the manure and decrease reactive oxygen content.[5] However, even though hydrothermal carbonizing manure renders the waste pathogen-free, it often leads to the unstructured of hydrochars with low surface area, making them less ideal for soil amendments.[6,7] Conversely, biochars produced from dry agricultural waste such as corn stover, cherry pits, and wheat straw appeared to have high surface areas, but the low concentrations of nutrients in most pyrolyzed biomasses requires separate fertilizer application.[8] Moreover, pyrolysis is not suitable for wet biomass streams such as cow manure due to the drying required as one of the pre-treatment.[9] Therefore, by proposing the novel integrated process that combines both HTC and pyrolysis, we can produce a soil amendment with the structural integrity of biochar and the nutrient retention capacity of a hydrochar.

In this thesis, we are investigating the optimal process pathway to produce nutrient-enriched soil amendments and biofuels using agricultural and animal waste. The two considered pathways are: 1. the combination of hydrothermal carbonization of wet animal waste + dry agricultural residues to produce solid hydrochars or 2. sequential hydrothermal carbonization of wet animal waste followed by co-pyrolysis of

hydrochars + dry agricultural residues to produce solid biochars using a set of representative biomasses common to Trentino-Alto Adige, Italy, the Black Sea Region, Turkey, and New York, USA.

Chapter 2: Background

In 2019, the United Nations estimated that 10 billion people would be living on Earth by 2050 (United Nations Department of Economic and Social Affairs, 2019). As the population rises around the globe, humans are challenged to grow food and sustainably generate cleaner energy to reduce greenhouse gas emissions and mitigate global warming. Along with the increasing demand for food, the agricultural waste that comes with food production would grow in the next century and eventually becomes an issue. The agriculture industry utilizes almost half of the Earth's natural resources, requiring more than 75% of the freshwater usage, encompassing more than 50% of the global reactive nitrogen load, and occupying around 40% of the total land area.[10–12] In the US, there are currently around 94 million dry tons of primary crop residues generated each year, which over 75% consist mainly of corn stover and wheat straw.[13] Conventional fertilizers are often abusively used to increase crop yields due to the limited amount of arable land. This over-fertilization not only causes an unbalance of nutrients in the soil but also contaminates water streams due to runoff. The nitrogen and phosphorus runoff from the excessive deployment of conventional fertilizers causes eutrophication of freshwater bodies. To address this issue, we need to develop sustainable soil amendments, which could be derived from abundant waste biomasses. Previous studies have shown that by using thermally upgraded biomasses as soil amendments, the nutrient uptake and water retention capabilities of plants and soil can be enhanced. To meet growing food demands in an environmentally responsible manner, we must improve the efficiency of water, nitrogen, and phosphorus use while converting most of the agricultural waste into renewable bioproducts.

Besides the agricultural food waste, the vast quantities of dairy products produced in the United States generate over 1 billion tons of animal manure, which contributes to over 7% of total greenhouse gas emissions in the US. Direct land-spreading of agricultural waste and animal manure is the primary management strategy due to their relatively high nitrogen and phosphorus content, making them suitable to be used as fertilizers.[1,3,14] However, these substrates are rich in bio-available carbon, which is highly biodegradable under ambient temperature by bacteria. This carbon loss reduces the efficiency of microbial activities and increases CO_2 emissions from the soil.

Not only does the growing population raise the need for food, but the globalization and industrialization also require more energy. According to the US Environmental Protection Agency, carbon dioxide and methane are the two most emitted greenhouse gases due to anthropological activities. Within the total greenhouse gas emissions, around 50% are electricity/heat production and agricultural related. While the CO_2 enhances the severity of global warming in the long term, CH_4 accelerates the process (Energy Defense Fund). The need for clean energy is urged to reduce climate change, where we can generate biofuels from biomass.

By converting agricultural waste to biofuels and stable nutrient-enriched soil amendments via integrated thermochemical conversion pathways, we can mitigate the environmental impacts on using conventional fertilizers and demonstrate a better approach towards sustainable agricultural waste management. In other words, the greenhouse gas emissions from land spreading strategy and the rapid nutrient leaching could be minimized. Furthermore, the utilization of biofuels produced using this method also demonstrates clean energy deployment around the world.

2.1 The two thermochemical processes to convert biomasses into biofuels and soil fertilizers

To utilize carbon and nutrients in agricultural waste, either biological (bacteria or enzymes) or thermochemical (heat or chemicals) processes can be used. As thermochemical processes often react faster and can generate different types of biofuel than biological processes, they are selected in this thesis. Several thermochemical pathways have been shown to convert biomasses to bioproducts, including hydrothermal carbonization/liquefaction, pyrolysis, combustion, and gasification. Although all thermochemical processes produce some amounts of solid, liquid, and gas, the yields and the characteristics of these three streams vary widely, depending on the conditions adopted. Since this thesis focuses on utilizing solids as soil amendments, hydrothermal carbonization and pyrolysis were selected based on their high solid yields.

2.1.1 Hydrothermal carbonization process, products, and applications

The thermochemical process of hydrothermal carbonization (HTC) is gaining industrial popularity for the conversion of wet biomasses into bioproducts[15]. The process occurs in sub-critical water at temperatures between 180-280 ^{o}C under autogenic pressure (saturated vapor pressure at the reaction temperature), with residence time varying from minutes to hours.[16] Three products are obtained: a liquid phase called AHL (aqueous HTC liquid), a solid phase known as hydrochar, and a gaseous phase mainly consist of CO_2[17]. The unprocessed hydrochar is usually separated from the liquid phase as a water-enriched slurry, often requiring dewatering for further utilization. The dried hydrochar can be utilized as a solid fuel (a

replacement for fossil fuels) in combustion applications for energy generation, as a feedstock for gasification, and some have proposed its use as a soil amendment.[18]

The main reactions that occur during HTC are dehydration, hydrolysis, decarboxylation, and aromatization.[19] The water, which is used as the reaction medium, removes the hydroxyl groups through dehydration, cleavages of esters and ethers group through hydrolysis, and removes carboxyl and carbonyl groups through decarboxylation.[20] These reactions generate polar organic compounds such as phenolic compounds and aldehydes, which acidify the media. At the same time, more aliphatic carbons are developed in the hydrochars, enhancing its biochemical recalcitrance in comparison to the starting feedstocks.[21] However, when using hydrochars as soil amendments, aliphatic carbons, in comparison to aromatic carbons, decompose fairly quickly under the ambient condition in the soil. The leached phenolic compounds and organic acids can drastically affect the soil properties, resulting in negative effects on plant and microbial responses.[22] Hydrochars could be used as solid fuels due to their higher energy densities as compared to their starting biomasses.[23]

2.1.2 Pyrolysis process, products, and applications

Pyrolysis is another thermochemical process used for the treatment of relatively dry substrates. Depending on the processing parameters, pyrolysis can be categorized into three types: slow pyrolysis, fast pyrolysis, and flash pyrolysis.[24] Since pyrolysis intensifies dehydration, wet biomasses are not suitable for this process due to the energy intensiveness for drying as a required pre-treatment. The main products of biomass pyrolysis are a solid phase (biochar), a liquid phase (bio-oil), and a gaseous phase, which is a non-condensable gas comprised mainly of CO, CO_2, CH_4, and H_2.[25]

The amount and composition of each stream varies based on the pyrolysis conditions. Yields of biochar, bio-oil, and bio-syngas are the highest for slow pyrolysis, fast pyrolysis, and flash pyrolysis, respectively. Thus, when the primary purpose of pyrolysis is to produce biochar for soil amendments, slow pyrolysis is preferred to maximize the solid yield.[26] At the industrial level, slow pyrolysis conditions are obtained in either fixed bed reactors or rotary kilns[27,28], in the absence of oxygen at temperatures between 300 - 700 ^{o}C at ambient pressure, usually for residence times greater than 450 seconds.[24]

During pyrolysis, thermal decomposition of biomasses takes place, cleaving more complex compounds such as cellulose, hemicellulose, and lignin into smaller compounds like aldehydes, acids, and ketones.[29] A series of reactions such as decarboxylation, decarbonylation, and dehydrogenation takes place to form biogas from the organic matter. A portion of the devolatilized organic matter re-condenses into a high-viscosity bio-oil, which contains, among other things, measurable amounts of water and compounds with oxygenated, acidic functional groups.[30] In the solid biochars, aromatic carbons with stabilized-structure form through aromatization. Because of such carbon condensation in the solid phase, biochar is thought to increase the soil cation-exchange capacity, to buffer its pH, and to prevent nutrients from leaching,[31] thereby enhancing crop yield.[32–34]

2.2 Physical properties of raw, hydrochars, and biochars that affect soil

Due to the different process temperatures and reaction media for HTC and pyrolysis, the structure of hydrochars and biochars vary widely. In the literature, both could be utilized as soil amendments to improve stability, microbial activities, nutrients, water

retention capacity, …etc.[35] The growth and yield of plants and crops are highly dependent on the soil properties such as nutrient availability, pH, electric conductivity, soluble and exchangeable Ca^{+}, and organic carbon. Although P, K, and N are naturally abundant mostly in rocks, the production cost of usable nutrients is increasing due to the increasing demand and the decrease in resources.[36] Prior studies on hydrochars and biochars show that these materials have the ability to retain nutrients in the soil, to adsorb and sequester heavy metals, and to serve as pH buffers.[37] Furthermore, the physical properties of the chars such as carbon, nitrogen, and hydrogen contents are also important when forming organic compounds (hydrocarbons) or determining the heating value if they are used as fuel applications.

Optimal soil pH is between 6.0 - 7.0 for most crops, as this value enhances crop yield by balancing the soil dynamic for plant nutrients uptake. An acidified soil causes nutrients deficiency in plants, produces toxic aluminum, and decreases microbial activities, eventually decreasing the crop yield. Electrical conductivity (EC) of the soil is another key parameter to determine the amount of minerals in the soil. The EC affects crop yield, crop suitability, nutrient availability, and microorganisms' activities, which is a factor that dictates the emission of greenhouse gases such as NOx, CH_4, and CO_2. The nutrients availability is directly related to the physical soil conditions such as pH and conductivity. According to Ketterings et al., nitrogen, phosphorus, potassium, sulfur, calcium, and magnesium have the highest available fraction in the pH 6.0-8.0 range.[38] Furthermore, if the soil is acidic (<6.0), ammonium could accumulate due to the low rates of nitrogen mineralization and decrease the efficiency of microbial activities.[39] C, H, O, N, P, K, Mg are the most common

inorganics found in biomass substrates. The concentrations of P, K, and N in the soil are generally correlated with crop yield.[40] Inorganic P typically exists as orthophosphate ($H_2PO_4^-$ and HPO_4^{2-}) in the soil depending on the soil's pH[41,42], which the plants can directly uptake. Potassium, another fundamental element for plant growth, improves water retention capability and increases drought resistance, and regulates the stomate, which controls the CO_2 uptake.[43] Potassium is needed to form protein and starch in plants.[44] Finally, inorganic nitrogen exists as nitrogen gas, nitrite, nitrate, and ammonium. Since nitrogen gas naturally exists in the atmosphere, the equilibrium of the atmosphere and the soil can be reached. Yet, organisms cannot directly use nitrogen gas due to the strong bond between the nitrogen atoms. Instead, nitrate (NO_3^-) and ammonium (NH_4^+) are the forms that can be easily utilized and are mostly found in soil. Unfortunately, rainfall and runoff can flush away part of the available nutrients causing nutrients deficiency to plants.[41] An overabundance or deficiency of plant nutrients can cause toxins to accumulate and the decrease in yield.[45,46]

Hydrochars are usually acidic (having pH below 6)[47,48], mainly due to the formation of acidic compounds such as formic, acetic, and lactic acids during the HTC process, which play important roles in dehydration and carbonization mechanisms.[49] Considerable amount of inorganics leached into the aqueous phase during the HTC process, resulting a lower ash content in hydrochars compare to biochars. The inorganics that remained on the chars include nutrients and toxic metals such as Si, K, Na, S, Cl, P, Ca…etc.[50] However, the use of hydrochars as soil amendments is questionable; some prior research has shown a reduction in nitrogen availability when

using hydrochars as soil amendments, which causes N deficiency in plants[51]. However, since the properties of hydrochar vary widely depending on processing parameters, there is potential to modify the N turnover by adsorption, mineralization, ammonification, nitrification, or immobilization.[51] By applying hydrochar as soil amendments, we could potentially adjust the amount of nitrogen uptake of the plants. In general, the oxygen-containing surface functional groups are the most contributors to create negative surface charges for the reduction of heavy metals through adsorption, especially the hydroxyl and carboxyl groups.[52]

Conversely, biochars, overall, are beneficial soil amendments, enhancing water and nutrient retention capabilities, plant growth, and fertilizer efficiency.[53] Biochars are weakly alkaline, which can be used to balance the pH of acidic soil in order to enhance crop yield.[54,55] They also decrease nitrous oxide leaching by adsorbing ammonium or ammonia.[56,57] Gasco et al. demonstrated that hydrochar and biochar from animal manure decrease the leaching of salts and metals, resulting in a lower conductivity compared to its raw form.[4] Although many prior studies report that utilizing biochars as soil amendments are beneficial, Lehmann et al.[58] caution that results are dependent on soil and biomass feedstock. For example, when applying biochars to forest lands, N availability to plants increases. On the other hand, no changes or decrease in N availability was observed when applying biochars on agricultural lands, possibly due to the type of soils and the volatile matter in the biochars.[59]

The two thermochemical processes have varying impacts on the formation of organic compounds. During HTC, the hydrolysis of cellulose causes the chains to break down to oligomers and glucose. The oligomers form the polymers and the skeleton of the

hydrochars while the glucose forms organic acids such as acetic, lactic, and formic acids. These acids lower the pH of the reacting media, which helps to break the C-C bonds and carbon rings. The substrate further undergoes dehydration, where C=O and C=C bonds are formed.[60] Since pyrolysis requires higher temperatures and occurs in a dry atmosphere, the oxygen and hydrogen in the biomasses significantly decrease in comparison to HTC. After the first drying step, the biomass undergoes carbonization and aromatization to form aromatic carbon rings.[61] Hydrocarbons, sulfur, nitrogen, phosphorus, halogens, and other carbonaceous derivatives could also be included in the organic compound, depending on the starting feedstocks.[62] Although biomasses and chars can have different organic compounds such as alkenes, alkynes, ethers, esters, carboxylic acids, ketones, aldehydes, anhydrides, and thiols, they vary widely across feedstocks.[63]

Good indicators of the capability of a char to hold water and to adsorb toxic meals are the char's surface area and surface functional groups.[64] The surface functional groups also determine the hydrophobicity of a sample. The presence of some hydrophilic functional groups in the hydrochar and biochar, i.e. carboxylic acid, methanol, aldehydes, anhydroglucoses, and furanoic compounds[65], influences the hydrophobicity of the material, promoting its suitability for adsorbing hydrophilic pollutants in soil applications. Raw biomasses usually have lower surface areas than hydrochars, which generally have a lower surface area than biochars. For biochars, the surface area often increases as the pyrolysis peak temperature and the residence time increase[66], since higher temperatures promote the development of aromatic C rings that enhance the surface area and pore development.[67] For hydrochars, the effect of temperature on the

surface area is minor.[68] Concerning the surface functional groups on the raw biomasses, hydrochars and biochars show distinct differences based on their different processes. More aliphatic carbons and fewer aromatic carbons are expected in the raw biomasses and hydrochar, compared to biochars.

Additionally, the intensities of functional groups in biochars from nearly all bands are also expected to decrease, even disappear at pyrolysis temperatures above 400 ^{o}C due to the decomposition of nonpolar aliphatic fractions.[69] According to Qambrani et al., more C=O and C-H functional groups were observed at a lower pyrolysis temperature (250 - 400 ^{o}C), while less ion-exchange functional groups were found in the biochar obtained at higher pyrolysis temperature (>400^{o}C) due to the dehydration and decarboxylation.

2.3 HTC and pyrolysis as pathways to renewable fuels

Beyond their potential use as soil amendments, both biochars and hydrochars could also be used as solid renewable fuels. While HTC produces minimal liquid fuel, pyrolysis does yield a liquid bio-oil. The energy content of the char, measured by its higher heating value (HHV), is a critical piece of information to gauge the potential for a given char to serve as a replacement for conventional solid fuels such as coal.[70] Traditional coal (bituminous or anthracite grades) provides approximately 33-35 MJ/kg of energy. [71] The typical HHV of raw biomass ranges between 10-30 MJ/kg on a dry basis[72]; HHV of hydrochars ranges between 24-30 MJ/kg[60]; HHV of biochars ranges between 10-35 MJ/kg, though it varies widely depending on mainly the carbon and hydrogen compounds.[73,74] The HHV is often directly measure via bomb calorimeter or calculated, but it can also be predicted if the amount of cellulose,

hemicellulose, and lignin is known. Kambo and Dutta[25] found that the HHV of cellulose and hemicellulose both are around 17 - 18 MJ/kg, whereas the HHV for lignin is 23 - 27 MJ/kg.

In addition to knowing the HHV, the elemental carbon, hydrogen, and oxygen content (determined via ultimate analysis) is useful to construct a van Krevelen diagram from the atomic O/C and H/C ratios, often used to gauge the suitability of a given fuel for combustion.[75,76] Calorific values can be estimated using the amount of C, H, N, and O in the chars.[77] The thermochemical reactions such as dehydration and decarboxylation influence the resulting O/C and H/C ratios, and as such the van Krevelen diagram is used to describe the degree and harshness of carbonization.[67] Raw biomasses usually have H/C and O/C ratios above 1.0 and 0.4, respectively. By going through the HTC and pyrolysis processes, the H/C and O/C ratios decrease. Decarboxylation, hydrolysis, and dehydration are the main contributors to reduce the O/C ratio.[15] Qi et al. observed that hydrogen depletes more than oxygen with higher temperatures during the carbonization process.[78] Basso et al. found that the oxygen content decreases when temperature and residence time increase, while the carbon content increases.[79] Likewise, pyrolysis significantly reduces the amount of hydrogen in the biomass due to dehydration and decarboxylation reactions, lowering the H/C ratio. As reported by Pariyar et al.[80], the lowering of the O/C ratio indicates aromatic rings forming that are graphite-like in structure, which results in biochars having higher stability in comparison to hydrochars and raw biomasses. While both thermochemical processes promote the lowering of low energy C-H and C-O bonds and enhancing the high energy C-C bonds, research shows that HTC has a more moderate effect on O/C and

H/C ratios while pyrolysis significantly reduces both as compared to the raw biomasses.[81]

During both wet and dry carbonization processes, organic compounds continuously release from the parent biomass matrix. The bio-oil produced via pyrolysis is highly oxygenated and enriched with water, as water is an inevitable by-product of devolatilization.[82] The most common compounds in bio-oil derived from lignocellulosic biomasses are lignin fragments, aldehydes, carboxylic acids, carbohydrates, phenols, furfurals, alcohols, and ketones.[83] Alkanes and alkenes also exist in the bio-oil depending mainly on operating temperature, duration, and physical composition.[84] The organic compounds in bio-oil depend on several factors: peak operating temperatures, temperature ramp rates, duration, and feedstocks. Although bio-oil is more environmentally friendly than conventional petroleum-based fuel, its heating value is often less than 50% of conventional petroleum-based liquid fuel.[85] Practically, due to the acidity and instability caused by the high oxygenated and hydrogenated compounds in the bio-oil, it is not suitable for liquid fuel substitution.[86] However, several upgrading techniques can reduce the amount of hydrogen and oxygen, which can upgrade the bio-oil to an alternative fuel source.[87]

By proposing the combination of the HTC and pyrolysis processes, we expect that the final product could be a better option for soil amendments, with the benefits of the hydrochar such as high nutrient concentrations as well as the biochars high surface area and alkalinity. This not only provides enough nutrients to the plants, stabilizes soil from organic and microbial activities, and enhances water retention capacity to

increase crop yield, but also effectively reduces farm waste by using them as the feedstocks.

Chapter 3: Materials and Methods

In light of a rising global population, our future supply of food and energy is tenuous, given the limited amount of agricultural lands and natural resources available. The overuse of conventional fertilizers is disrupting the natural ecosystem, from unbalancing soil dynamics to polluting freshwater sources. The direct application of agricultural waste as substitute fertilizers, coupled with the increasing use of fossil fuels, is increasing greenhouse gas emissions. Therefore, identifying green and renewable soil amendments and energy sources is essential to promote a sustainable society. This thesis focuses on exploring optimal thermochemical pathways, discussed in the next chapter, to produce soil amendments and renewable fuels from waste biomass that can replace conventional fertilizers by combining hydrothermal carbonization and pyrolysis.

3.1 Feedstocks

Three biomasses were selected to represent the agricultural and dairy industries equally relevant to three regions: Central New York, USA; Trentino-Aldo Adige, Italy; Black Sea Region, Turkey: corn residue (CS), grape marc (GM), and cow manure (CM). Corn residue is a high-nitrogen waste left from agricultural production in upstate New York, around Trentino, and in the growing agricultural industry in the Black Sea region. Corn accounts for over 95% of the total feed grain produced in the United States (USDA). Grape marc was selected as it is a by-product of the wine-making industries of both Ithaca and Trentino, and the expanding grape-producing regions of the Black Sea. Cow manure is a nitrogen and phosphorus enriched wet biomass source, representing the intensive dairy operations in all three regions. Corn

residue was harvested from a Cornell University farm, while the grape marc and the cow manure were obtained from a local winery and dairy farm in Trento, Italy. The cow manure was stored in plastic containers at -4 ^{o}C in a freezer and defrosted directly before use.

3.2 Hydrothermal Carbonization (HTC) of Biomass

HTC was performed in an in-house built 50 mL stainless steel (AISI 316) batch reactor at the University of Trento described in previous literature.[7,88] The temperature of 220 ^{o}C with a residence time of 1 hour was used to mimic industrially relevant conditions. The reactor was charged with a 0.2:1 (dry) biomass to water (B:W) ratio, fully submerging the biomass while leaving comparable volumes in the reactor[88].

In addition to the pure raw corn stover, grape marc, and cow manure, two-component mixtures of these singular biomasses were made by combining [CS + CM] and [GM + CM] at 3 different weight percentages (25%, 50%, and 75%) measured on an analytical balance to the ±0.1 mg. The list of the substrates and the corresponding abbreviations for each biomass and blend are shown in Table 1. The purpose of blending these biomasses is two-fold. First, neither corn stover nor grape marc has sufficient intrinsic moisture content to be hydrothermally carbonized on its own; additional water must be added to carbonize them individually. However, cow manure contains greater than 90% water, such that co-carbonizing CS or GM with CM lowers the need for freshwater use. Secondly, cow manure on its own does not produce stable hydrochars – such chars are quickly transformed into fine dust that could present an inhalation hazard upon land application. We hypothesized that by co-carbonizing cow manure with these lignocellulosic biomasses that we could improve the hydrochar

stability. Hydrochars are denoted using the letters "HC" before the feedstock abbreviation.

Table 1. Agricultural waste feedstocks and their mixtures used for HTC

Feedstock	Raw Abbreviation	Hydrochar Abbreviation
Raw corn stover	CS	HC CS
Cow manure	CM	1hr HC CM; 2hr HC CM*
Raw grape marc	GM	HC GM
Raw CS 25 % + CM 75 %	CS25CM75	HC CS25CM75
Raw CS 50 % + CM 50 %	CS50CM50	HC CS50CM50
Raw CS 75 % + CM 25 %	CS75CM25	HC CS75CM25
Raw GM 25 % + CM 75 %	GM25CM75	HC GM25CM75
Raw GM 50 % + CM 50 %	GM50CM50	HC GM50CM50
Raw GM 75 % + CM 25 %	GM75CM25	HC GM75CM25

* An additional set of CM hydrochar was produced for co-pyrolysis with raw biomass using a 2L reactor over 2hr as detailed below

The setup of the system can be found in previous literature.[89] Prior to the reaction, the reactor was purged by flushing nitrogen (Airliquide Alphagaz 1™). The sample and deionized water were added into the reactor to the 0.2 B:W ratio (±0.01g). The system was then directly heated to 220 °C. The residence time started right after the system reached 220 °C. Followed by the 1hr reaction time, the reactor was placed on a stainless-steel disk at -24 °C while the air was blown into the cooling coil surrounding the reactor. After room temperature was reached, the valve connected to a graduated cylinder was opened to allow gas us to collect gas. The produced hydrochar was recovered by filtering through 45 μm cellulose filter paper and dried in a well-ventilated oven at 105°C until constant mass. The hydrochar solid mass yield was calculated by the mass ratio between hydrochar and feedstocks (dry basis); gas mass yield was calculated from the gas volume by assuming 100% CO_2 produced, as the

typical CO_2 molar fraction is greater than 95%[90]; the liquid mass yield was determined by the remaining fraction.[7]

In addition to the 1-hour hydrochars, cow manure was also carbonized at 220 ^oC for 2 hours in a 2L stainless steel (AISI 316) reactor with the same process described above. The 2 hr HC CM was to be used in co-pyrolysis experiments, as described in the following section.

3.3 Pyrolysis of Biomass

The pyrolysis and co-pyrolysis experiments were performed at Cornell University using an MTI 2" horizontal fixed bed furnace. A series of nine biochars were fabricated as detailed in Table 2. The three feedstocks consisted of CS, GM, and the 2 hr HC CM. Blends of 25:75, 50:50, and 75:25 by weight of CS + 2hr HC CM and GM + 2hr HC CM were prepared prior to pyrolysis by weighing the components on an analytical balance into glass vials and vortex mixing the vials to ensure homogeneity.

Table 2. Agricultural waste feedstocks and their mixtures used for Pyrolysis

Feedstock	Biochar Abbreviation
CS	BC CS
2hr HC CM	BC CM
GM	BC GM
Raw CS 25 % + 2hr HC CM 75 %	BC CS25CM75
Raw CS 50 % + 2hr HC CM 50 %	BC CS50CM50
Raw CS 75 % + 2hr HC CM 25 %	BC CS75CM25
Raw GM 25 % + 2hr HC CM 75 %	BC GM25CM75
Raw GM 50 % + 2hr HC CM 50 %	BC GM50CM50
Raw GM 75 % + 2hr HC CM 25 %	BC GM75CM25

Nitrogen was used as the carrier gas, supplied by a nitrogen generator (ESA) at 150 mL/min with a minimum purity of 99.5% (confirmed by an Extorr residual gas analyzer). The initial biomasses were weighed and loaded into an alumina combustion

boat until 2/3 full to prevent heat and mass transfer limitations.[91] The boat was then placed in the heating zone in the center section of the furnace, shown in Figure 1(A). The temperature profile in Figure 2 comprised an isothermal stage (110 ^{o}C) to drive off residual moisture, followed by heating at 10°C/min to 600 ^{o}C, and maintained at that temperature for one hour. Two vacuum flasks (Chemglass) served as cold traps connected in series to condense bio-oil from the exiting gas using dry ice + ethylene glycol as cooling media. The pyrolysis system setup is shown in Figure 1, where (B) is the furnace temperature controller, (C) and (D) are the first and second cold traps, respectively, (E) is the gas exit point, where the remaining volatiles and nitrogen were released, and (F) is the vacuum flasks filled with ethylene glycol and dry ice.

Figure 1. Pyrolysis system setup at Cornell University

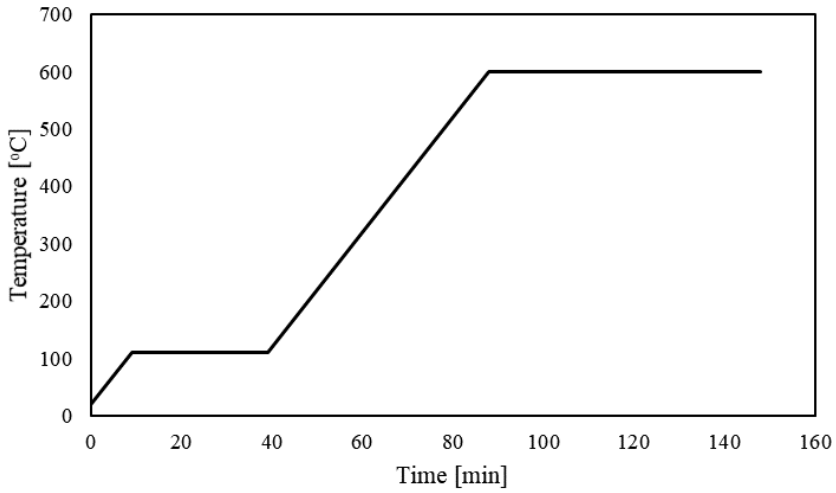

Figure 2. The temperature profile of the pyrolysis process

The condensed volatile matter (bio-oil) deposited in the cold traps was dissolved in 20 mL of dichloromethane (DCM). Dewatering of the bio-oil was performed to remove the moisture generated during the pyrolysis process. Anhydrous magnesium sulfate was added to the 0.1 mL mark in a 1.5 mL autoclavable microcentrifuge tube, to which the extracted bio-oil was added to the 1.3 mL line. The microcentrifuge tubes were shaken for 1 min and centrifuged at 2000 rpm for 3 minutes or until supernatant and solids separated. The supernatant was extracted and stored at -4 °C.

3.4 Proximate analysis and Thermal stability

Thermogravimetric analysis was used to determine the proximate analysis and gauge the thermal stability of the materials in a TGA 5500 (TA Instruments) using N_2 (Airgas) and air as carrier gases. The proximate analysis determines the amount of Moisture (Moist.), Volatile matter (VM), Fixed carbon (FC), and Ash in the samples, in this case following ASTM standards.[92–95] All samples were individually sieved to 106-500 μm using 3" ASTM certified brass sieves on a motorized shaker (CertifiedMTP) for 16 minutes, following ASTM standards.[96] Particles of this size

were chosen to prevent heat and mass transfer limitations[91,97] and to ensure homogeneity before further analyses. An analytical balance (Shimadzu) was used to weigh out the samples to 4-6 mg before loading them onto platinum sample pans on the TGA 5500. The proximate analysis of as-received (ar) basis and dry basis (db) were carried out.

The moisture content was determined by raising the TGA temperature to 110 ^{o}C and holding for 30 minutes at this temperature under nitrogen gas[93]. The nitrogen flow rate was set to 100 mL/min for both mass and balance flows to ensure an inert chamber. As-received moisture content was calculated using Equation 3.4.1, where m_0 is the initial sample loading mass, and the m_{dry} is the sample mass after drying at 110 ^{o}C and 30 minutes.

$$\%_{Moist,ar} = \frac{m_0 - m_{dry}}{m_0} * 100\% \quad (3.4.1)$$

The as-received volatile matter ($\%_{VM,ar}$) content was determined by raising the temperature to 910 ^{o}C and held isothermally for 30 minutes at 910 °C under nitrogen[94], calculated using Equation 3.4.2, where m_{FC} is the mass of fixed carbon, m_{ash} is the mass of ash. $m_{FC} + m_{ash}$ is the mass remaining after devolatilization at 910 °C under nitrogen.

$$\%_{VM,ar} = \frac{m_{dry} - (m_{FC} + m_{ash})}{m_0} * 100\% \quad (3.4.2)$$

The as-received ash ($\%_{ash,ar}$) content was determined by raising the temperature to 950 ^{o}C and holding for 30 minutes under air for complete oxidation[95], which was calculated using Equation 3.4.3. m_{ash} is the mass of the sample after complete oxidation.

$$\%_{Ash,ar} = \frac{m_{ash}}{m_0} * 100\% \quad (3.4.3)$$

Lastly, the as-received fixed carbon ($\%_{FC,ar}$) content was calculated as the remaining weight fraction of the sample using Equation 3.4.4.

$$\%_{FC,ar} = 100 - \%_{Moist} - \%_{VM} - \%_{ash} \quad (3.4.4)$$

The proximate analysis is reported on a dry basis as moisture content could be affected due to the environment. The dry basis was calculated using Equations 3.4.5 - 3.4.7.

$$\%_{VM,db} = \frac{\%_{VM,ar}}{\%_{VM,ar}+\%_{FC,ar}+\%_{ash,ar}} \quad (3.4.5)$$

$$\%_{FC,db} = \frac{\%_{FC,ar}}{\%_{VM,ar}+\%_{FC,ar}+\%_{ash,ar}} \quad (3.4.6)$$

$$\%_{Ash,db} = \frac{\%_{Ash,ar}}{\%_{VM,ar}+\%_{FC,ar}+\%_{ash,ar}} \quad (3.4.7)$$

In addition to the proximate analysis, derivative thermogravimetric (DTG) curves were constructed using the TG data by taking its derivative of weight change with respect to time. The DTG curves region was taken from 110 – 910 ^{o}C (pyrolysis) as most of the organic matter devolatilized during this temperature. The curves represent the thermal stability of the biomasses, indicating the relative devolatilization rates of different biomasses. The DTG curves were plotted using Equation 3.4.8 and 3.4.9, where x(t) is the normalized conversion rate at time t, m_t is the mass at time t, $m_{dry,initial}$ and $m_{dry,end}$ are the masses at 110 ^{o}C and 910 ^{o}C. $\frac{dx}{dt}$ is the change of conversion rate in 1/min, $x_{t1,}$ and x_{t2} are the conversion rates at t_1 and t_2, which t_1 and t_2 represent two different consecutive times starting right after 110 ^{o}C.

$$x(t) = (m_{dry,initial} - m_t)/(m_{dry,initial} - m_{dry,end}) \quad (3.4.8)$$

$$\frac{dx}{dt} = (x_{t1} - x_{t2})/(t_1 - t_2) \quad (3.4.9)$$

3.5 Ultimate analysis and Higher heating value (HHV)

In addition to the information provided through proximate and thermal analyses, the ultimate analysis gives us the contents of both organic and inorganic carbon, hydrogen, nitrogen, and oxygen. The ultimate analysis was performed on a CE-440 elemental analyzer (Exeter Analytical Inc.) via steady-state combustion analysis using oxygen (99.99%, Airgas) as the fuel and helium (99.99%, Airgas) to carry the combusted products through the analytical system to the atmosphere in accordance with ASTM D3176[98]. Samples, in the range 1-3 mg, were weighed using a microbalance (Mettler Toledo, 0.1 mg precision) and loaded in a consumable tin capsule and manually placed into the sample chamber connected to the combustion tube. The sample was then combusted in oxygen at 975 ^{o}C, and the produced gas reduced at 650 ^{o}C. Acetanilide (>99.9% purity) was used as the standard material to calibrate the instrument. Ash was calculated from the proximate analysis, and the oxygen content was determined by difference. Sulfur was not measured as it was only present in trace amounts (<0.2% by wt.) in the raw biomasses.[99] All data is reported on dry ash-free basis.

The higher heating values of the samples were calculated using Dulong's Equation, Equation 3.5.1[100], where %C, %H, and %O are weight percentages determined via the ultimate analysis on dry basis.

$$HHV\ \left[\frac{MJ}{kg}\right] = 33.5 \cdot \%C_{db} + 142.3 \cdot \%H_{db} - 15.4 \cdot \%O_{db} \quad (3.5.1)$$

3.6 pH and electrical conductivity

When used as soil amendments, hydrochars and biochars can alter the soil dynamics such as pH and conductivity.[101–103] A SevenExcellence benchtop pH/conductivity meter (Mettler Toledo) was used to measure the pH and electrical conductivity (EC). pH calibrations of pH 4, pH 7, pH 10, and conductivity calibration (12.88 mS/cm) solutions purchased from ThermoFisher Scientific were used before every measuring batch. The water was obtained from a Milli-Q water purification system (Millipore Sigma) with minimum resistivity of 18.2 MΩ. Blank Milli-Q water was used for each measuring batch as the baseline since the pH and conductivity of the water fluctuate daily.

pH and conductivity analyses were carried out following a modified International Biochar Initiative (IBI) method to account for the low availability of some samples.[104] The IBI method states that the standard biochar to water ratio is 1:20, whereby 1 gram of biochar is suspended in 20 mL of water, equilibrated, and the water's pH and EC measured. To determine the effect of dilution on the measured pH and corresponding sensitivity, five different biomass to water ratios (1:20, 1:40, 1:60, 1:80, and 1:100, m:v) were tested using nine initial biomasses (CS, 2hr HC CM, GM, and six raw + 2hr HC CM mixtures). The variation in the results of pH was minimal, and due to the limited amount of HC and BC, a modified method was employed using 1:100 biomass to water ratio to determine the pH and conductivity. Approximately 0.05 g of each sample was weighed on an analytical balance (Shimadzu) into a 15 mL falcon tube with 5 mL of water. The tube was shaken at 200 rpm for 90 minutes then centrifuged

at 2500 rpm for 5 minutes at room temperature. The pH and conductivity were directly measured in the falcon tube using the probes.

3.7 Surface Area Analysis

The pore volume and surface area of soil amendments are properties that influence the total adsorption of undesired products such as heavy metals and organic compounds, the nutrient cycle, microbial activities, and the water retention capacity of the soil.[105] Surface area and pore volume measurements for samples were obtained from N_2 physisorption at 77 K using a 3-Flex surface area analyzer (Micromeritics) following the modified methods of IBI[104] and ASTM D6556[106]. Prior to analysis, samples were dried in a laboratory oven overnight at 110 °C to remove surface moisture before degassing. Degassing was performed in glass bulbs that were evacuated before thermal treatment. A degassing temperature of 110 °C was used for raw biomasses and hydrochars, and 200 °C was used for biochars. The maximum degassing temperature for each sample was selected to improve the degassing efficiency without causing significant thermal degradation. Samples remained degassing until reaching an outgassing rate of $1.0 \cdot 10^{-3}$ mmHg/min, which was below the recommended threshold of $2.5 \cdot 10^{-3}$ mmHg/min that is considered sufficient by the instrument manufacturer for an accurate isotherm measurement. Typical outgassing times for biomass samples were between 20 and 48 hours. After degassing, samples were analyzed by obtaining 23 isotherms points ranging between a relative pressure of 0.0001 to 0.99. The multipoint BET fitting was performed using 5 isotherm points ranging between relative pressures of 0.05 and 0.30. Analysis of the N_2 isotherms was performed using the Brunauer Emmett and Teller (B.E.T.) method to determine the

surface area of representative samples. The BET fitting equation is provided in Equation 3.7.1.

$$\frac{P}{V_a(P_0-P)} = \frac{1}{V_m C} + \frac{C-1}{V_m C} * \frac{P}{P_0} \quad (3.7.1)$$

where P is the manometer pressure, P_o is the saturation vapor pressure of nitrogen, V_a is the cumulative pore volume, V_m is the volume of nitrogen per unit mass that covers one monomolecular layer, and C is the BET constant. The V_m and the C constant can be found by plotting $\frac{P}{P_0}$ on the x-axis versus $\frac{P}{V_a(P_0-P)}$ on the y-axis from the slope and the intercept, respectively. [106,107] The cumulative volume of nitrogen adsorbed (V_N) per unit mass of a sample can be calculated using Equation 3.7.2 at each isotherm point $\left(\frac{P}{Po}\right)$.[106] The total pore volume of a material is determined at the point closest to the relative pressure of 0.99, processed in the software provided by Micromeritics.

$$V_N = \frac{Volume\ of\ Nitrogen\ for\ each\ dosing\ in\ cm^3}{sample\ mass\ in\ g} \quad (3.7.2)$$

The C constant can be used to evaluate the relative error between single and multipoint BET, typically at $\frac{P}{P_o} = 0.3$. If the C constant has a value <20, the BET method is considered not a good fit for the isotherm.

3.8 Fourier Transformed Infrared Spectroscopy (FTIR)

The surface functional groups of the soil amendments impact the adsorption capability of pollutants by altering the surface charge. In addition, microbial activities, which impact plant nutrient uptake and greenhouse gas emissions, are also influenced by the surface functional groups of the amendments. Fourier transform infrared (FTIR) spectroscopy was used to identify the presence of functional groups on the surface of the organic materials.

FTIR spectra were collected on a Vertex 70 FTIR Spectrometer (Bruker) with a KBr beam splitter analyzed using diffuse reflectance (DR) mode. The pellet (~200 mg) was prepared with approximately 1% of biomass samples with 99% of IR grade KBr (ThermoFisher Scientific) and gently ground and mixed using a mortar and pestle. The mixed powder was pelletized using a pelletizer (Diameter of 13 mm) and a benchtop press (Carver) at 5 tons. The spectra were obtained between the wavenumber range of 4000-600 cm^{-1}, a resolution of 8 cm^{-1}, and with defaulted scans. The DR-FTIR spectra were processed using the OPUS spectroscopy software by Bruker Inc.

3.9 Inorganic extraction

Using hydrochars and biochars as soil amendments can influence the crop yield due to the HC and BC nutrient content.[108] Elements such as P, K, and Mg are critical to plant growth. Other beneficial nutrients that promote microbial activities include Zn, Cu, Ni, and Co. Contradictorily, toxic metals such as Cd, Cr, and Pb are not desirable in the soil.[109] The bioavailable inorganics of initial biomasses, hydrochars, and biochars were determined using the Mehlich-III (M-III) extraction method[110]. All solutions were made and stored in polypropylene containers and plastic pipettes to prevent contamination from borosilicate glassware and stainless steel. Trace metal grade HNO_3 and ACS reagent grade for other chemicals were purchased from ThermoFisher Scientific.

The M-III solution was prepared following the Mehlich protocol. Since the original Mehlich method[110] was prepared for approximately 2000 samples, a modified scaled-down method was used. Stock solution - Approximately 6 mL of DI (MilliQ) water was added to a 10 mL polypropylene volumetric flask with 1.389 g of NH_4F and well

mixed; sequentially, 0.7306 g of Ethylenediaminetetraacetic acid (EDTA) was added into the flask and topped to 10 mL with DI water. The stock solution was mixed until no suspended solids were observed. Working solution – Approximately 40 mL of DI water was added to a 50 mL polypropylene volumetric flask with 1.000 g of NH_4NO_3 and well mixed; 0.200 mL of stock solution was sequentially added and mixed. 0.575 mL of CH_3COOH (glacial) and 0.041 mL of HNO_3 were added into the flask. Lastly, the flask was topped to 50 mL with DI water. Tuning of the working solution to the pH of 2.5 ± 0.1 was performed using 1 M HCl (if pH>2.5) or 1 M NH_4OH (if pH<2.5). A 1:100 (m:v) biomass to extract ratio was used. Approximately 0.05 g (±10%) of the material was added to a 15 mL falcon tube with 5 mL of M-III solution and shaken at 200 rpm for 5 minutes under room temperature. The M-III digestate was filtered through a $0.45\mu m$ syringe filter into a new 15 mL falcon tube. Hot plate carbon digestion using concentrated nitric acid (70%, Trace metal grade) was adopted to remove the residual carbon in the solution that could potentially promote mineralization and affect the readings on ICP-MS. A micropipette was used to transfer 0.75 mL of the M-III digestate into an autoclavable 1.5 mL microcentrifuge tube along with 0.5 mL of 70% concentrated nitric acid. The microcentrifuge tube was left open in the fume hood on a hot plate at 40 ^oC overnight. The digestate level was monitored constantly, and 70% nitric acid was added when needed to ensure complete digestion. After the carbon digestion, 65% of the nitric acid strength was assumed, which was diluted to a 2% nitric acid matrix required by the ICP-MS.

The organic-free M-III digestates were analyzed via an ICP-MS 2030 (Shimadzu). Argon (Airgas) was used as the plasma source and helium (Airgas) as the gas for

collision cells. Before analyzing the samples, calibrations with 0.1, 1, 5, and 10 ppb of each element stated above were performed with a calibration standard purchased through High Purity Standards. The collision cells were turned on to mitigate the possible interference of different elements.

3.10 Analysis of pyrolysis bio-oil

The bio-oil analysis was performed via Gas Chromatography – mass spectrometry (Shimadzu GCMS-QP2010SE) coupled with an AOC-20i+s autosampler (Shimadzu). A Rxi-5Sil MS column (Restek) of 0.25μm thickness, 0.25 mm inner diameter, and 30 m length was installed. This column was selected to reduce the background signal generated by the column stationary phase, therefore producing a better signal to noise ratio. The bio-oil described from the previous section was directly transferred into GC vials after returning to room temperature and analyzed without further sample preparation. Before each batch experiment, automatic tuning was performed. The injection volume was set to 1 μL. The initial column oven temperature was set to 40 ^{o}C with an injection temperature of 250 ^{o}C. The injection mode was set to split with a 1:20 split ratio. Helium (Airgas) was used as the carrier gas with the GC flow control mode set to pressure. A pressure of 49.5 kPa was used while other parameters such as total flow, column flow, and purge flow were automatically filled. The ion source temperature was set to 230 ^{o}C with an interface temperature of 250 ^{o}C. The MS was set to Electron ionization (EI) mode at 70 eV. The solvent cut time was at 2 minutes. Table 3 shows the two heating rates used across three stages, as lower temperature ramp rates significantly reduced the shifting of the baseline.

Table 3. GC parameters used for bio-oil analysis

Stages	Ramp rate (°C/min)	Final Temp (°C)	Hold time (min)
0	-	40	5
1	1.75	150	5
2	1.75	250	10
3	2.50	300	10

After the sample (bio-oil) was injected into the gas chromatograph and vaporized, the vapor was carried by the He gas through the column. Different compounds in the mixture interact differently with the stationary phase of the column, therefore traveling at different speeds and exiting the column at different times. When the compounds leave the column, they entered the mass spectrometer, where a high energy beam of electrons is applied to the molecules, ionizing them and breaking them into fragments. The mass of the charged fragments was divided by the charge applied to get the mass to charge ratio (m/z). These charged particles then traveled through the quadrupole mass analyzer and reached a detection plate where the relative abundance of the compounds was measured. The MS was set to scan across from 15 – 600 m/z to include both lighter and heavier compounds. The mass of the 40 most abundant compounds (40 peaks with the largest area in chromatogram) were matched in the GCMS post-run analysis software provided by Shimadzu using the NIST17 database with a minimum similarity of 80%. The parameters set for the MS are shown in Table 4.

Table 4. MS parameters used for bio-oil analysis

	Start time (min)	End time (min)	Acq. mode	Event time (sec)	Scan speed (μ/sec)	Start m/z	End m/z
1	6	120	Scan	0.3	1428	15	400
2	120	170	Scan	0.3	1428	200	600

Chapter 4: Results and Discussion

While both hydrothermal carbonization (HTC; subcritical heating in water) and pyrolysis (heating in an inert atmosphere) convert carbonaceous wastes to hydrochars and biochars, respectively, neither alone is a perfect solution to biomass waste management. Some biomass wastes, such as cow manure, are rich in nutrients such as P and K, yet their high moisture content precludes the use of pyrolysis. Other biomass wastes, such as corn stover, are relatively dry compared to cow manure and are lignocellulosic materials, ideally suited to pyrolysis. By proposing an integrated thermochemical process that combines either co-HTC of animal manure and dry agricultural residues to concentrate P and K, or co-pyrolysis of pre-carbonized manure and raw dry agricultural residues to develop high surface areas, structurally sounds biochars, we can reduce agriculture's environmental impact while recovering solid and liquid biofuels as nutrient-enriched soil amendments and possible renewable fuels.

4.1 Physical properties of raw biomasses, hydrochars, and biochars

The physical and chemical properties of raw, hydrothermally carbonized, and pyrolyzed biomasses were characterized to determine the potential for each material to serve as a soil amendment or solid fuel. The three wastes – grape marc, corn residue, and cow manure – were chosen as agricultural residues that represent many regions across the globe, including Central NY, USA, Trentino-Alto Adige, Italy, and the Black Sea Region of Turkey.

4.1.1 Raw biomasses

The raw corn residue consists of leaves and stalks collected from a farm in Central NY, USA. The raw grape marc consists of 50% dried grape skin and 50% dried grape seed collected from a winery in Trento, Italy. The cow manure was also retrieved from a farm located in Trento. The initial moisture content of each biomass was measured as-received, the two dry biomasses were dried and stored in sealed plastic containers, while the cow manure was placed in plastic containers and frozen, as-received, at -4°C to prevent degradation.

4.1.2 Hydrochars

Hydrothermal carbonization is a common technique to upgrade wet biomasses such as cow manure. Nutrients tend to concentrate in the solid hydrochars, and the hydrochars usually exhibit longer-term stability (less susceptible to microbial and thermal degradation), which is an advantage when using them as soil amendments. The yields from HTC/co-HTC processing of the raw feedstocks are shown in Table 5, where the yields are reported in weight percentages. All biomasses yielded between 65-75% solid hydrochar, which is in line with literature values for similar feedstocks.[79,81]

Table 5. Solid, gas, and liquid yield of hydrochars in weight percentages

	Solid [wt. %]	Gas [wt. %]	Liquid [wt. %]
HC CS	70.0	6.8	23.2
1hr HC CM	72.9	3.1	24.1
2hr HC CM	65.7	7.0	27.3
HC GM	69.2	5.4	25.4
HC CS25CM75	73.4	4.9	21.7
HC CS50CM50	69.0	5.9	25.1
HC CS75CM25	68.2	6.5	25.3
HC GM25CM75	69.2	5.1	25.7
HC GM50CM50	71.1	3.5	25.4
HC GM75CM25	66.8	3.4	29.8

4.1.3 Biochars

Pyrolysis was performed on the raw corn residue, raw grape marc, and the 2hr HC cow manure to demonstrate an integrated thermochemical pathway. Since pyrolysis is suitable for dry biomasses (usually less than 20% moisture), using HTC to pretreat cow manure reduces the overall energy input as hydrothermal carbonization imparts a somewhat hydrophobic nature to the hydrochars, making it possible to separate the solid cow manure hydrochar from the aqueous phase via simple gravity filtration. The yields from pyrolysis and co-pyrolysis of the three raw/HTC feedstocks and their six mixtures are shown in Table 6. The cow manure has the highest solid biochar yield of 53.6 %, and the raw corn stover has the lowest biochar yield of 30.3 %. As observed from Table 6, the mixtures with 2 hr HC CM showed a high solid yield.

Table 6. Biochar yield from pyrolysis and co-pyrolysis

Starting feedstocks	Biochar Yield [wt. %]
CS	30.3
2hr HC CM	53.6
GM	35.4
CS25CM75	48.5
CS50CM50	42.5
CS75CM25	35.9
GM25CM75	49.9
GM50CM50	43.9
GM75CM25	40.6

4.1.4 Proximate Analysis

The proximate analysis of the three initial biomasses (CS, GM, and 2hr HC CM) and their mixtures are shown in Table 7. Since moisture can be affected by the surrounding environment such as atmosphere and sample handling, data are reported on a dry basis. Testing was done in triplicate, and the values are reported as averages with standard deviations. The hydrochars overall showed a decrease or negligible change in volatile matter, and a slight (<10%) increased in fixed carbon and ash compared to the initial biomasses. This could be explained by the low temperature (220 ^{o}C) and the short residence time of HTC, in which the cellulose, hemicellulose, and lignin do not fully decompose. Biochars, in general, have the highest fixed carbon with an average increase of 34% and the lowest volatile matter, with an average decrease of 50% as compared to the initial biomasses. Biochars also have approximately twice the amount of ash and half the amount of the volatile matter when compared to raw biomasses and hydrochars. In addition, hydrochars have significantly less ash than biochars, which agrees with previous literature, due to some minerals in the hydrochars dissolving and being washed out into the water media during the HTC process.[111] Among CS, HC CM, and GM, corn stover has the highest volatile matter, 2hr HC cow manure has the

highest ash content, and grape marc has the highest fixed carbon fraction. The results showed consistency with previous publications on the proximate analysis.[112–114] The distribution of volatile matter, fixed carbon, and ash observed in Table 7 do not vary much with respect to their mixtures.

Table 7. The volatile matter, fixed carbon, and ash weight percentage of raw biomasses, hydrochars, and biochars via thermogravimetric analysis

		VM %	FC %	Ash %	VM stdev.	FC stdev.	Ash stdev.
CS	Raw	75.56	15.28	9.16	0.06	0.72	0.71
	HC	67.87	21.80	10.33	1.07	0.56	0.53
	BC	14.94	60.30	24.76	0.40	1.14	0.81
GM	Raw	67.62	28.61	3.77	0.81	0.69	0.38
	HC	63.29	33.19	3.53	0.81	0.49	0.68
	BC	11.10	81.11	7.78	0.10	1.23	1.26
CM	1hr HC	59.01	15.63	25.36	1.63	0.82	0.97
	2hr HC	59.24	17.32	23.44	0.94	0.27	0.67
	BC	17.40	36.19	46.41	0.47	3.17	3.63
CS25CM75	Raw	62.79	17.52	19.69	0.31	0.36	0.58
	HC	63.02	17.20	19.77	0.57	0.30	0.37
	BC	17.91	40.08	42.01	0.88	2.22	3.08
CS50CM50	Raw	65.77	17.51	16.72	0.54	0.31	0.59
	HC	63.08	19.31	17.60	0.85	0.42	0.58
	BC	16.37	48.04	35.59	0.19	0.99	1.02
CS75CM25	Raw	70.74	16.71	12.55	0.64	0.31	0.40
	HC	64.82	21.37	13.81	1.18	0.65	0.75
	BC	14.44	54.15	31.41	0.86	2.39	2.17
GM25CM75	Raw	59.58	20.28	20.14	1.28	1.48	1.44
	HC	59.31	19.74	20.94	0.64	0.35	0.43
	BC	16.71	44.94	38.35	0.25	1.61	1.63
GM50CM50	Raw	62.54	21.93	15.54	0.93	1.78	2.61
	HC	62.50	22.29	15.21	0.60	0.34	0.60
	BC	15.20	54.13	30.66	0.59	1.32	1.56
GM75CM25	Raw	66.68	23.79	9.53	2.35	2.29	0.11
	HC	64.39	25.98	9.63	1.59	2.25	1.38
	BC	13.61	65.34	21.04	0.36	1.09	1.35

4.1.5 Ultimate analysis

The ultimate analysis is reported in Table 8 on dry ash-free (daf) basis. The carbon determined both organic and inorganic compounds, such as mineral carbonates. The hydrogen was also accounted for both organic and inorganic compounds in the sample, and the nitrogen content was assumed to be within the organic compounds of the sample. The oxygen was calculated from the remaining fraction. The ultimate analysis not only gives the relative stability of the material from the ratio of carbon, hydrogen, and oxygen, it could also be used as a cursor to estimate the quality of biomass.

Table 8. The ultimate analysis of raw biomasses, hydrochars, and biochars on dry ash-free basis on weight percentages

		C %	H %	N %	O %
CS	Raw	67.08	5.81	1.08	26.03
	HC	61.37	5.86	1.59	31.18
	BC	90.44	1.19	1.91	6.46
CM	1hr HC	66.02	6.48	3.12	24.38
	2hr HC	67.28	6.22	3.36	23.14
	BC	88.47	0.77	4.17	6.59
GM	Raw	59.22	5.92	1.81	33.05
	HC	71.79	5.91	1.92	20.37
	BC	90.55	1.19	2.21	6.06
CS25CM75	Raw	67.44	6.09	2.74	23.74
	HC	71.66	6.22	2.71	19.40
	BC	82.03	0.58	3.29	14.10
CS50CM50	Raw	67.30	5.99	2.15	24.56
	HC	64.95	6.19	2.30	26.56
	BC	88.90	0.73	2.61	7.76
CS75CM25	Raw	67.16	5.90	1.60	25.35
	HC	64.72	6.02	1.91	27.35
	BC	90.61	0.65	2.28	6.46
GM25CM75	Raw	65.32	6.09	2.92	25.67
	HC	70.29	6.53	1.57	21.61
	BC	80.50	0.71	3.44	15.36
GM50CM50	Raw	63.26	6.01	2.51	28.22
	HC	71.49	6.53	2.53	19.46
	BC	90.12	0.74	3.03	6.11
GM75CM25	Raw	61.42	5.94	2.15	30.49
	HC	73.98	6.37	2.20	17.46
	BC	90.01	0.87	2.64	6.48

Interestingly, HC CS shows a decrease in carbon and an increase in oxygen compared to its feedstock. This was unexpected because HTC should increase the carbon content while decrease the hydrogen and oxygen contents. The 2hr HC CM indicated a slight increase in carbon and a slight decrease in oxygen compared to the 1hr HC CM. The HC GM showed a 12 % increase in carbon and a 13% decrease in oxygen to the GM. The decrease of oxygen and hydrogen and increase of carbon was consistent with the HTC temperature and longer residence time described in the literature.[115] Corn stover and grape marc biochars demonstrate high carbon contents (80-90%, by wt.) while the oxygen and hydrogen significantly decreased, possibly due to the inert atmosphere during pyrolysis process in comparison to the water media for HTC, which limited the interactions between oxygens and hydrogens to the sample. However, the cow manure biochar showed a decrease in both carbon and oxygen, suggesting that the pyrolysis process drove off the organics that contained carbon and oxygen, which can be further verified through the surface functional group analysis in the upcoming section.

As can be seen in Figure 3, the H/C atomic ratio of hydrochars and raw biomasses are similar (1.0-1.2), while some of the O/C ratios overlapped. Along with the relatively similar atomic C, H, and O ratios of hydrochars and raw biomasses compare to biochars. It is suggested that only dehydration and decarboxylation occurred during HTC. And since the HTC temperature was low and the duration was short, the effect on reducing the oxygen was not that significant. The reactions described previously led to the decrease in oxygen and the increase in carbon, resulting in the lower H/C and O/C ratios compare to raw biomasses. Conversely, biochars have H/C and O/C ratios that are <0.6 and <0.4, conforming to the IBI definition of biochar. The low H/C

and O/C ratios also indicate high stability in comparison to hydrochars and raw biomasses. Chars used as soil amendments with high stability are less likely to biodegrade under ambient conditions and affected by microbial activities.

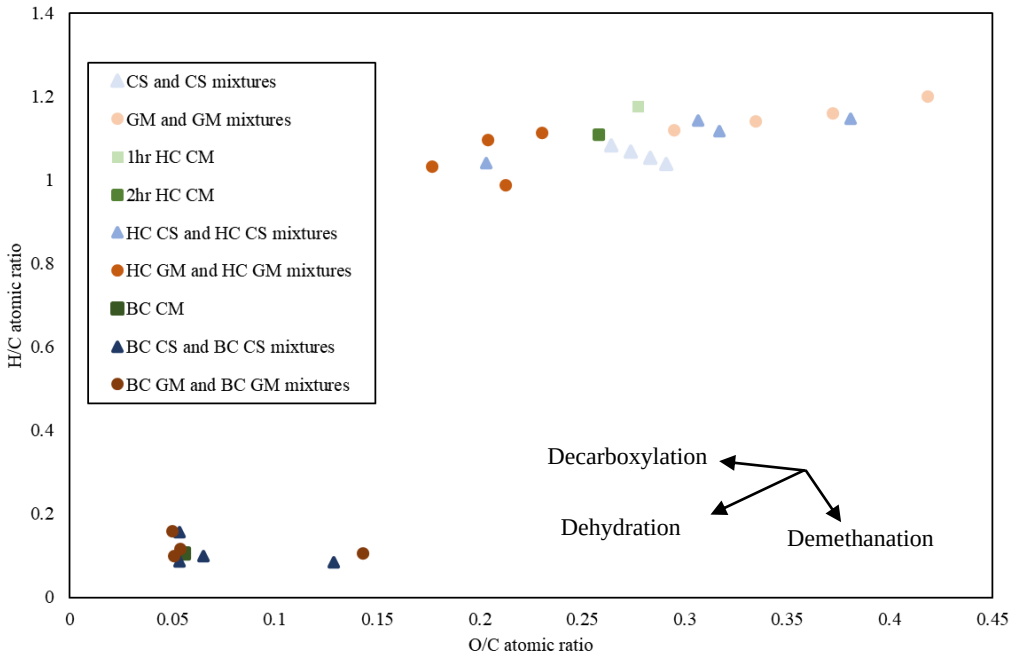

Figure 3. van Krevelen diagram of raw biomasses, hydrochars, and biochars

4.1.6 pH and conductivity effects on the water when exploiting raw biomasses, hydrochars, and biochars as soil amendments

Soil pH and conductivity not only influence soil's microbial activities, pesticide interactions, mobility of heavy metals, and corrosivity but also impact the crop yield. A modified IBI protocol was used to assess the pH and conductivity of biomasses. This protocol employs a 1:20 biomass to water ratio (m:v) for both measurements. However, due to the limited quantities of samples, a modified IBI method with a 1:100 biomass to water ratio was adopted in this work. To ensure the accuracy of the results by this modified method, a series of different loading concentrations (1:20-1:100, biomass to water, m:v) using raw/2hr HC CM biomasses was done, the results of

which are shown in Figure 4 and Figure 5. The results indicated that the loading concentrations range from 1:20 to 1:100 have little effects on the change of pH and has a close to linear relationship on the conductivity.

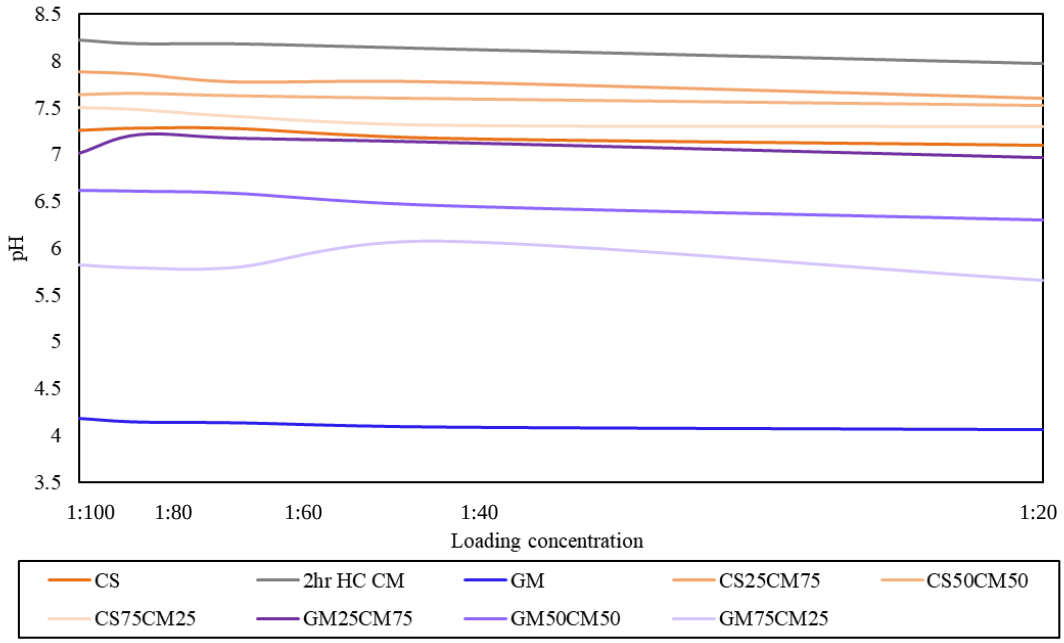

Figure 4. Measured pH using 1:20-1:100 biomass to water (m:v) ratios

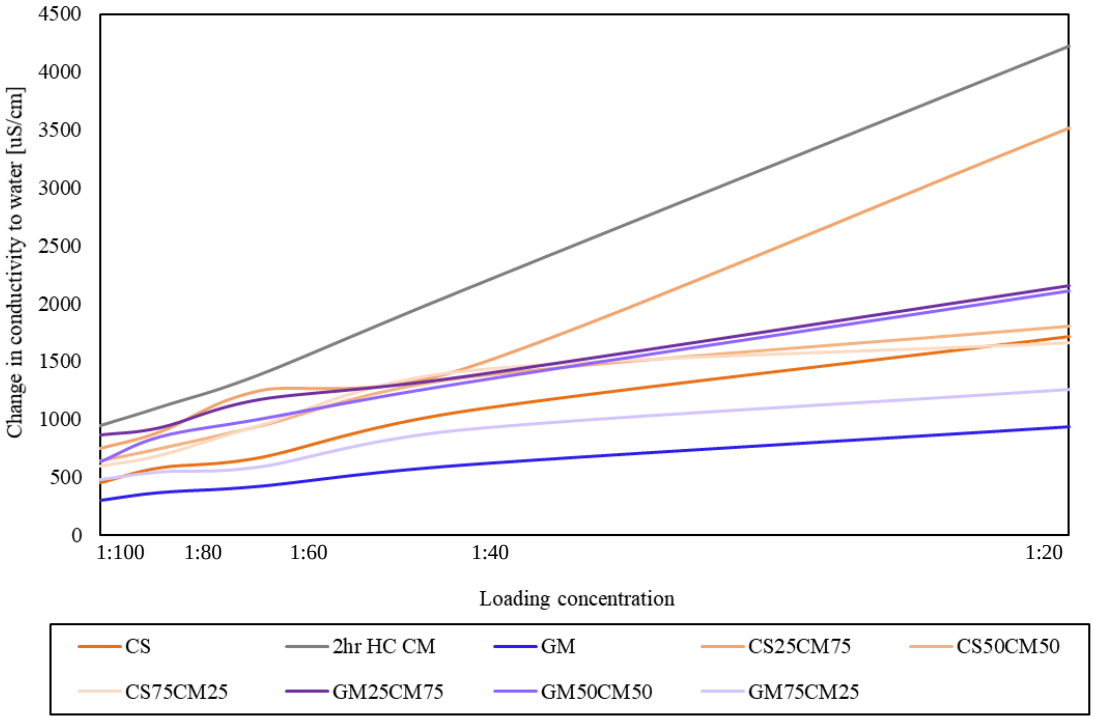

Figure 5. Change of EC using 1:20-1:100 biomass to water (m:v) ratios

Ultra-pure water (Millipore) with a resistivity of at least 18.2 MΩ was used to ensure no minerals are presented in the solution that would affect the measurements. Since the CO_2 in the atmosphere and the temperature fluctuate daily, a blank (100% water) was measured to be used as the reference point. Therefore, the results shown in Table 9 are reported in regards to the baseline (blank).

Table 9. The pH and the conductivity (μS/cm) measured from initial biomasses, HC, and BC using a 1:100 (m:v) sample to water ratio. (Blank at pH=8.789, conductivity=2.788μS/cm)

	Initial biomasses								
	CS	GM	CM	CS25 CM75	CS50 CM50	CS75 CM25	GM25 CM75	GM50 CM50	GM75 CM25
pH	7.26	4.18	8.23*	7.88	7.64	7.50	7.01	6.62	5.82
Cond.	464.10	307.50	954.96*	754.57	651.03	603.90	868.70	640.26	491.63
	HC								
pH	5.65	5.34	8.11**	7.43	7.01	6.57	7.73	6.76	6.22
Cond.	457.75	191.93	864.28**	820.69	674.56	485.73	698.06	551.78	317.40
	BC								
pH	10.36	10.82	11.05	10.67	10.69	10.54	10.96	11.30	10.79
Cond.	735.34	552.08	1099.56	928.01	1075.50	908.02	1013.71	1099.48	830.99

* indicates 2hr HC CM, **indicates 1hr HC CM

According to Table 9, all biochars have higher pH than the water blank, suggesting more OH^- ions than H^+ ions are presented in the water, indicating alkalinity of the biochars. The hydrochars and initial biomasses are acidic as their pH is lower than the blank. The findings are consistent with published literature.[47,111,116] Grape marc shows the lowest pH, indicating the most H^+ ions released across all samples, which is possibly due to the high oxygenated and hydrogenated surface functional groups. The CM (1hr HC, 2 hr HC, and BC) demonstrates the greatest change in conductivity across samples, possibly due to the ions leached out from the cow manure. GM (raw, HC, and BC), on the other hand, shows the least change in conductivity most likely due to the high carbon content, which stabilizes the surface functional groups and reduces the leaching of ions. According to the United States Department of Agriculture (USDA), the optimal soil conductivity for food crops is in the range of 1000 μS/cm – 5700 μS/cm (or 1 dS/m – 5.7 dS/m).[117] Excess or insufficient

conductivity in the soil leads to a decrease in crop yield. Additionally, the optimal soil pH is 6.0 - 7.0, which lowers the dissolution of heavy metals, leading to corrosions of concrete and pipes, and increases the microbial activities contributing to the breakdown of available nutrients.[118] Hence, biochars could be used to raise the pH of the soil, and hydrochars can be used to lower the soil pH while both of them can increase the conductivity of the soil to optimize the microbial activities.

4.1.7 Surface area effects on the water and nutrient retention capabilities

The results of the surface area using nitrogen adsorption are shown in Figure 6 reported in m^2/g. Both corn stover and grape marc show similar surface areas (<5 m^2/g). The corn stover and grape marc hydrochars demonstrate an increase in surface area of 100-250% compared to their raw forms. However, the HTC blends see little change in surface area, most likely limited by the presence of the cow manure. When 25% of cow manure is mixed with either corn stover or grape marc, the surface area dropped by over 35%. The low surface area on the cow manure is probably due to its compositions such as lipids and nitrogen-contained compounds, in which no real structure was developed, leading to the failure of pore formation hence decreasing the surface area. Secondary char formation during the HTC process could also be another cause besides the unstructured cow manure. Lucian et al.[119] demonstrated that spherical structured secondary char would precipitate on the primary char mainly from the furfural produced during the sequential hydrolysis, dehydration, and isomerization in HTC with the intermediate acids presented in the media. These spherical secondary chars deposited on the surface and block the pores, resulting in low surface areas.

The corn stover and cow manure biochars showed an increase in surface area compared to their hydrochars and raw materials. The grape marc biochar has a lower surface area than its hydrochar, which was unexpected. Biochars in the literature generally show an increase in surface area due to its reactions, in which devolatilizing of organic matters takes place during the process, releasing the pores in the material.[120] However, some groups observed a decrease in surface area at higher pyrolysis temperatures greater than 500 ^{o}C, potentially due to the collapse of pore structures, which led to the low surface area.[121,122] Tag et al. discovered that low surface area was obtained for low-ash materials.[123] This observation was consistent in the low-ash grape marc and high-ash cow manure biochars. The low biochars surface areas seen in Figure 6 could be due to the high particle densities, the shrinkage of the particles, and the ash blocking the pores during the pyrolysis process.[116,124], if the pores released by the volatile matters are dead-ended, no contributions would be made towards increasing the accessible surface area.[125]

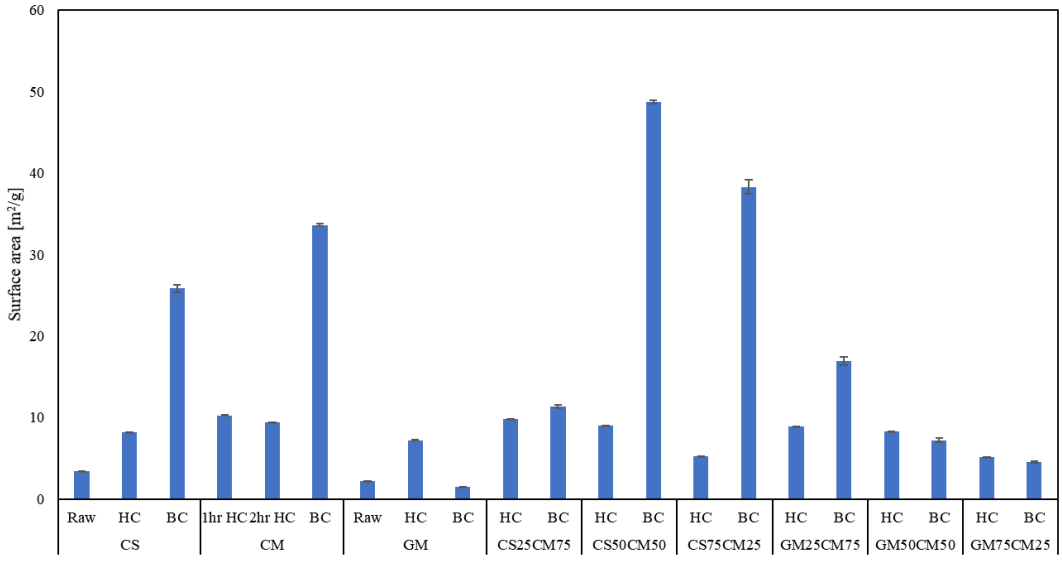

Figure 6. The surface area of initial biomasses, hydrochars, and biochars obtained through the BET method by nitrogen adsorption.

Figure 7 shows the total pore volume at a relative pressure of approximately P/P_0 = 0.99, reported in cm^3/g. As shown, the total pore volumes of corn stover and cow manure increase in both hydrochar and biochar forms, while grape marc presented a low total pore volume compare to corn stover and cow manure. The cow manure biochars have relatively high total pore volume compare to corn stover and grape marc shown in Figure 6. The low pore volumes in grape marc biochar could also be influenced by the low degassing temperature (200 ^oC) to prevent thermal degradations of the samples.

Although reporting surface area using BET theory is often considered as a standard in carbon science, it might not be a good fit in this case since the surface areas were minimal. In other words, the underlying theory of BET uses a monolayer of nitrogen to adsorb onto the sample. If the sample has more effects on multilayer adsorption between particles, the reading of the nitrogen adsorbed would be minimal. Although N_2 isotherms from the sorption instrument are reproducible for biochar samples, the BET analysis leads to a relatively poor fit, which could be attributed to the low sample surface area. Overall, it may be said that the cow manure has the highest surface area, and the grape marc has the lowest surface area using BET theory. The high surface area of cow manure recommends that using cow manure as soil amendments would have a better effect on retaining water, nutrients, and limiting heavy metal leaching[33] in the soil from the surface area perspective.

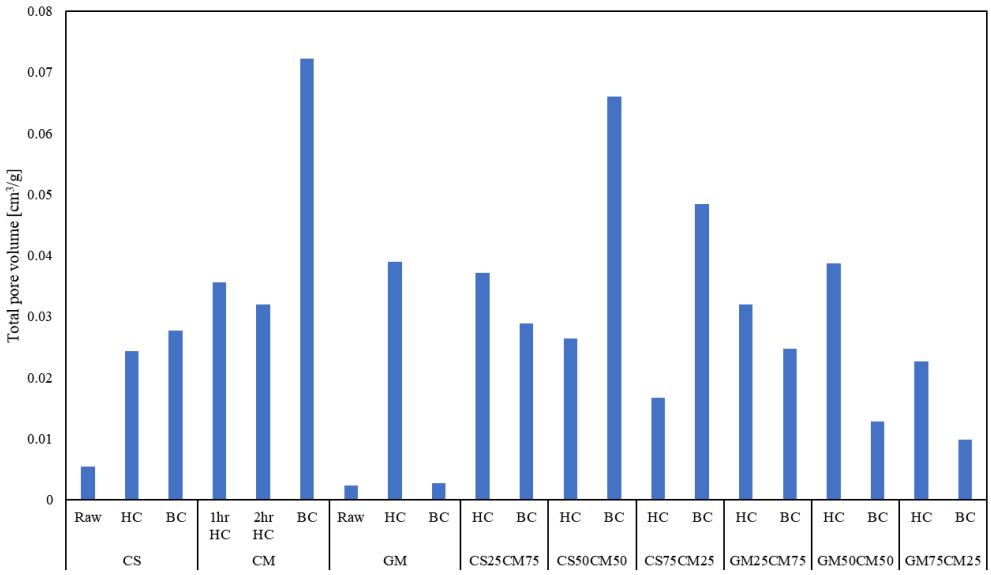

Figure 7. The total pore volume of initial biomasses, hydrochars, and biochars at a relative pressure of 0.99

4.1.8 Surface functional groups that affect soil dynamics and heavy metal adsorption

The surface functional groups of soil amendments play a vital role, which is linked to the mineralization of carbon and nitrogen, resulting in the change of nutrient availability.[126] Fourier-transform infrared spectroscopy (FTIR) was used to qualitatively assess the presence of different surface functional groups on the surface of the specimens. The normalized infrared spectra of the biomass feedstocks, their hydrochars and biochars are shown in Figure 8, Figure 9, Figure 10, and Figure 11. Since the carbon content plays a major role in the development of the surface functional groups, only GM25CM75 and GM75CM25 were selected for measurements across the mixtures. The correspondence between wavenumbers in the range of 4000 - 500 cm^{-1} and associated surface functional groups is extensively studied in the literature, a summary of which is shown in Table 10. Generally, the peaks between 4000 cm^{-1} and 1500 cm^{-1} are easily distinguishable and are usually due to the stretching vibration of diatomic units. However, many different functional

groups may exist in the fingerprint region between 1500-500 cm^{-1}, and the separation of these individual functional groups is challenging due to overlapping.

Table 10. Typical functional groups exist in biomass with their assigned wavenumbers

Wavelength (cm^{-1})	Types of bonds	Classification	Reference
3600-3100	O-H	Stretching hydroxyl groups	[127,128]
2850, 2920	C-H	Aldehydes, Alkanes, Alkenes, Alkynes	
1740	C=O	Aldehydes, Ketones, Carboxylic acids	[128,129]
1630, 1510, 1420	C=C	Aromatic compounds	[130,131]
1385	C-H	Stretching vibration of -CH2	[132]
1261, 1161	C-O	Alcohol, ethers, esters, carboxylic acids, anhydrides	[133]
1101, 1031	-	Ash	[134]
875, 805	C-H	Aromatic out-of-plane bend	[128]

Across Figure 8, Figure 9, Figure 10, and Figure 11, all raw CS, raw GM, and 2hr HC CM, and the mixtures show significant amounts of alcohol functional groups. Compared to the initial biomasses, hydrochars have more complex aromatic compounds and oxygen-containing functional groups such as ester, ether, and acid. The increase in the intensities range 1600 - 1000 cm^{-1} was expected since the HTC was performed in an acidic aqueous solution. The organic matters dissolved in the HTC media containing carbon, oxygen, and hydrogen recondensed back to the surface of the chars, resulting in more functional groups. Grape marc hydrochars showed more aromatics compared to corn stover hydrochar and cow manure hydrochars. The increase in C=C bonds in grape marc was possibly due to its higher lignin content in comparison to corn stover presented in the previous section.[135]

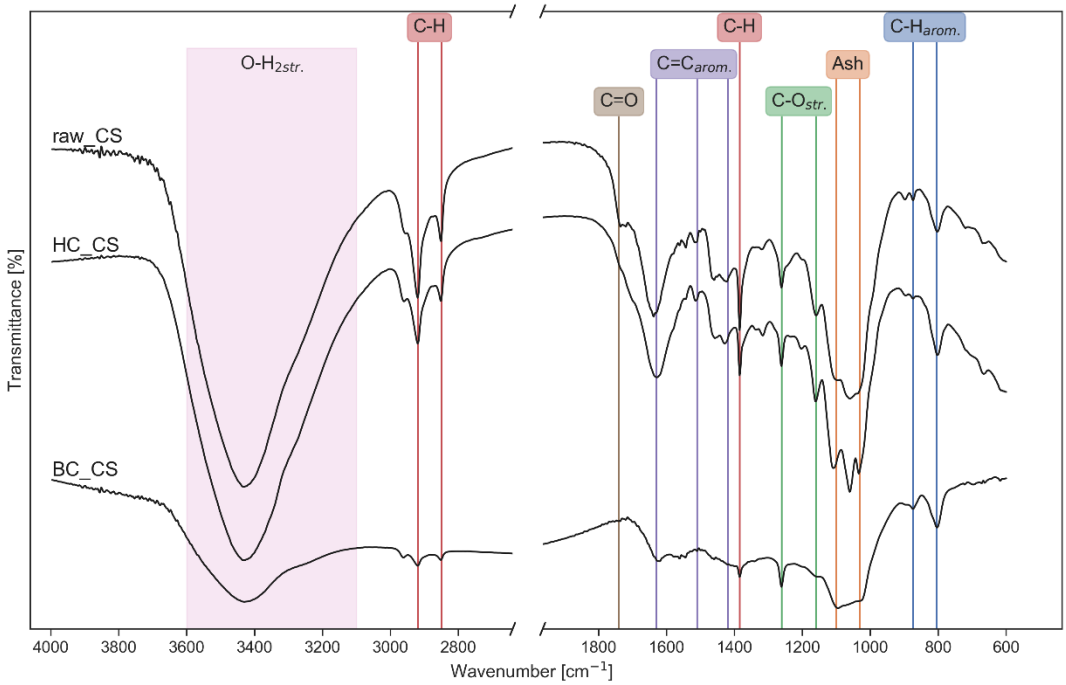

Figure 8. FTIR spectrum of raw, HC, and BC corn stover

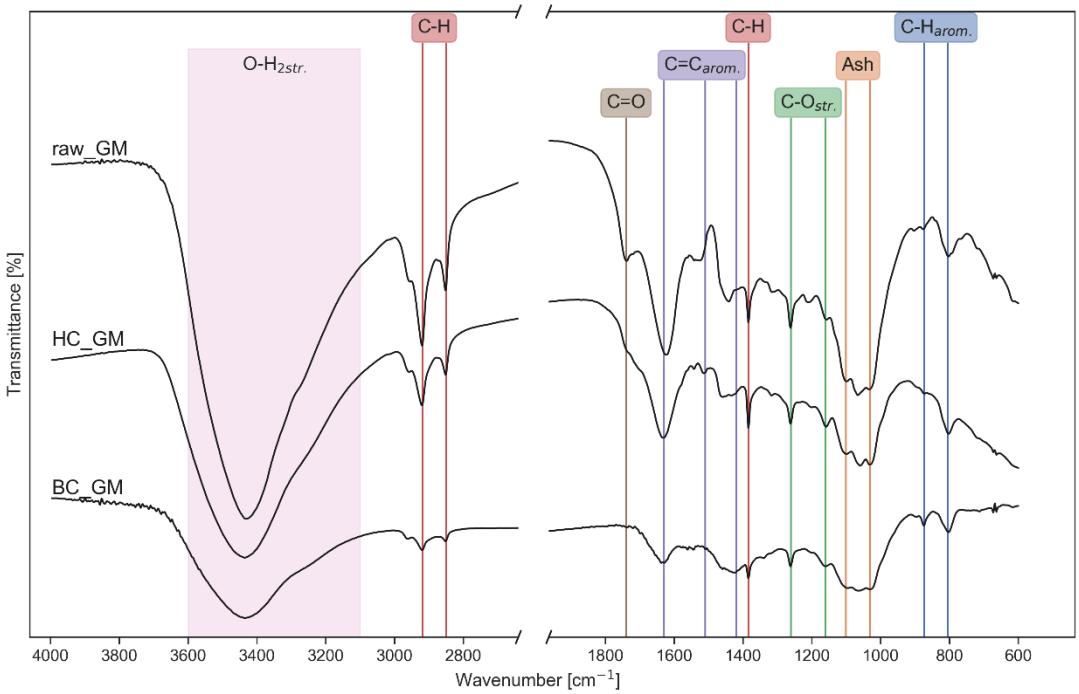

Figure 9. FTIR spectrum of raw, HC and BC grape marc

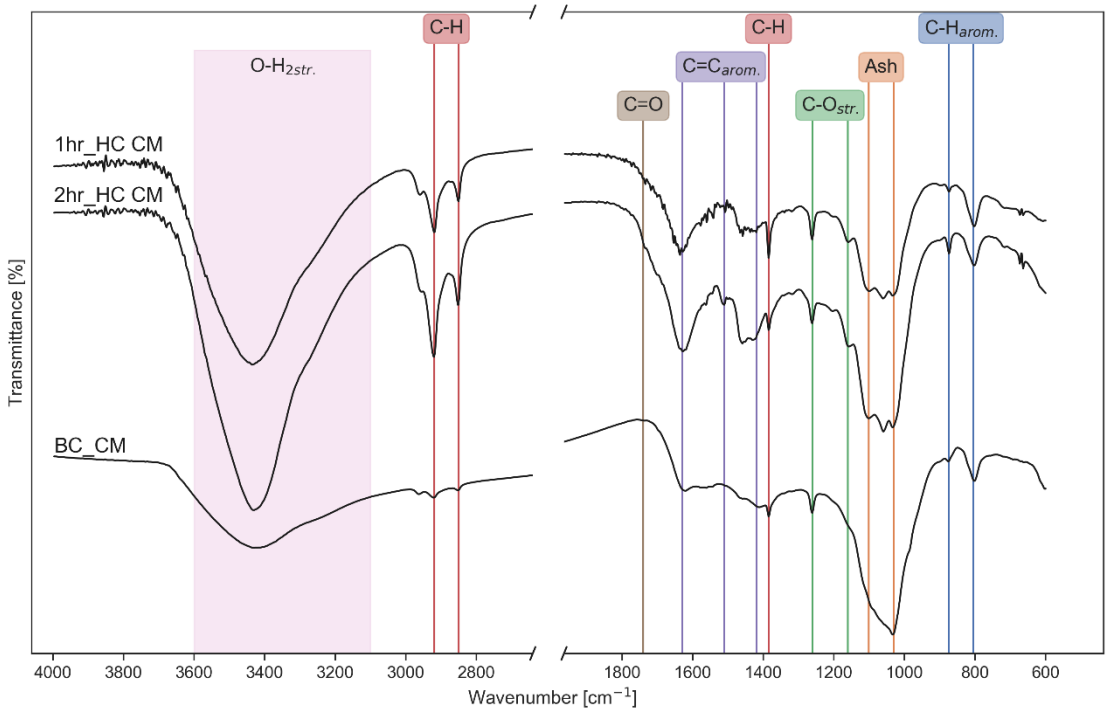

Figure 10. FTIR spectrum of HC and BC cow manure

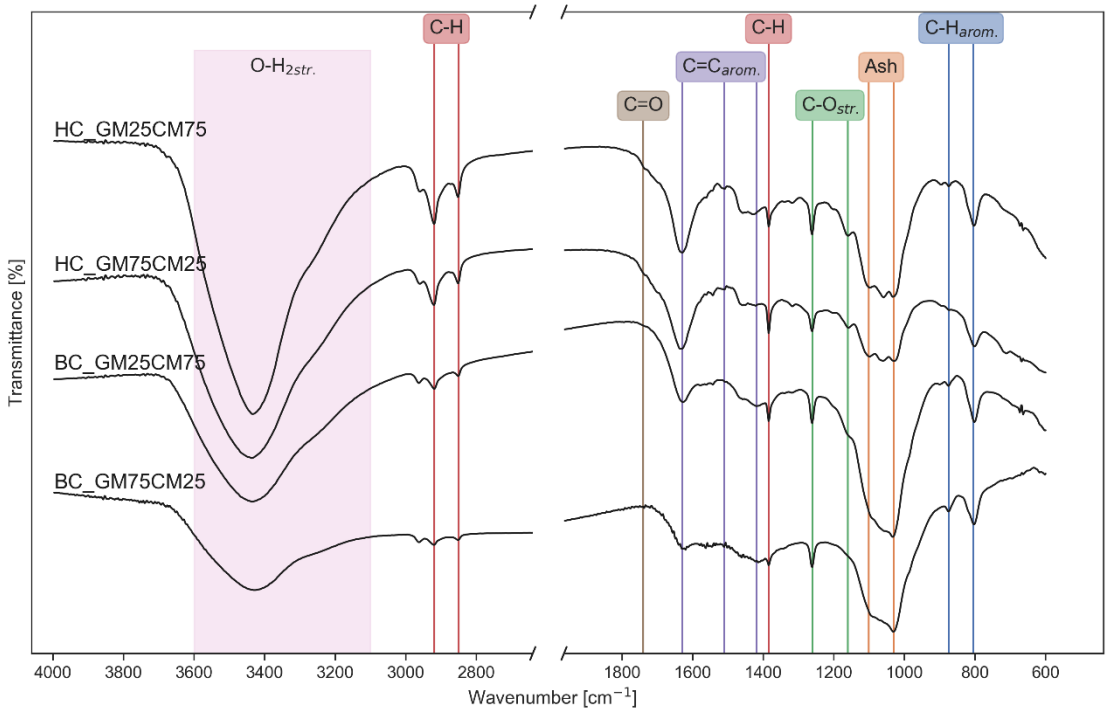

Figure 11. FTIR spectrum of HC and BC mixtures

Biochars showed lower intensities in the alcohol groups and aliphatic carbons compared to raw biomasses and hydrochars. The lower peaks in between those wavelengths suggest that aliphatic carbons and alcohol groups transformed into more stable functional groups, perhaps alkenes and aromatics at lower wavenumbers. The peaks at 1101 and 1031 cm^{-1} in the cow manure were attributed to the ash content.[134] Although the raw biomasses show more functional groups at higher wavenumbers (C-H aliphatic and O-H stretching), hydrochars show higher intensities across the 1700-900 cm^{-1} region (oxygen-containing and aromatic compounds), due to the recondensing of organic matters in the HTC process. Biochars overall have lower intensities compare to hydrochars and raw biomasses, due to its devolatilization of organic matters during the pyrolysis, which also devolatilize most of the surface functional groups containing oxygen and hydrogen. This suggests that the raw biomasses and hydrochars could have similar particle surface charges, which is significant to the adsorption of heavy metal cations in the soil. Oxygen-containing functional groups, such as hydroxyl groups, aldehydes, esters, and ethers, can create negative charges on the particle surface, which promote the immobilization of heavy metals with positive charges.[136] Past studies show that the oxygen-containing functional groups increase in hydrochars compared to the feedstocks; pyrolysis reduces the presence of surface functional groups[137], which was consistent with the FTIR spectra shown above and the O/C atomic ratios in the ultimate analysis shown in the previous section. The polar functional groups containing oxygens and hydrogens on the hydrochars may also increase the water retention capability, based on electrostatic interactions and the hydrogen bonds.[137] Therefore, the enrichment of the

functional groups in hydrochars, in comparison to the biochars, makes hydrochars better soil amendments to both immobilize heavy metals and enhance water retention capacity.

4.1.9 Nutrients (P, K, Mg) and heavy metals in raw biomasses, hydrochars, and biochars when utilizing as soil amendments

The hydrochars' and biochars' nutrient concentrations vary depending on the processing media, temperature, and feedstocks.[108,138] Nutrients such as phosphorus (P), potassium (K), and magnesium (Mg) in the soil help plants fight diseases, expand the roots for growth, aid in the process of photosynthesis, and enhance the adaptability in a drought environment.[43] Microbial activities, which facilitate the transport of these nutrients, can also be enhanced by the addition of nitrogen and carbon. Heavy metals in soil can bioaccumulate in plants and crops and be harmful to human organs when ingested. As reported in the literature, the amount of bioavailable nutrients are relatively low in biochars compared to their feedstocks, which may be explained by the accumulation of the nutrients when releasing the volatile organic matter during pyrolysis.[137] Mehlich-III extraction was performed to assess the bioavailable nutrients in the samples. By determining the bioavailable nutrients, we can better understand the nutrient utilization as soil amendments, and compare them to the IBI[104] maximum allowed threshold for nutrients.

Bioavailable P, K, Mg, along with Cd, Cr, Co, Cu, Pb, Mo, Ni, Se, Zn were measured following IBI[104] protocol for determining the range of maximum allowed threshold for biochar materials. The bioavailable nutrients and heavy metals are shown in Table 11, where the units are in mg of inorganics per kg of sample.

Table 11. Bioavailable inorganics via Mehlich-III extraction in initial biomasses, hydrochars, and biochars reported in mg of nutrients per kg of sample

	Initial Biomasses								
	CS	CM	GM	CS25 CM75	CS50 CM50	CS75 CM25	GM25 CM75	GM50 CM50	GM75 CM25
K	1294.3	2894.2	1932.0	2730.0	2190.7	1906.7	3427.1	3035.5	2401.8
Mg	295.7	1011.0	79.2	994.0	788.1	490.7	1144.8	690.8	366.1
P	158.6	1330.0	233.8	1241.8	943.7	478.7	1545.8	978.7	583.1
As	N/A	0.1	N/A	0.1	0.1	N/A	0.1	0.1	N/A
Cd	N/A	N/A	N/A	N/A	N/A	N/A	N/A	N/A	N/A
Co	N/A	N/A	N/A	N/A	N/A	N/A	N/A	N/A	N/A
Cr	2.8	1.8	3.1	3.0	1.7	1.7	3.3	1.8	1.7
Cu	10.6	N/A	14.7	11.0	N/A	N/A	11.9	2.3	3.7
Fe	14.4	142.7	16.4	129.6	103.6	38.3	166.3	84.4	53.6
Mn	1.6	31.8	1.0	29.4	23.2	9.6	34.6	19.5	11.1
Ni	4.1	4.4	4.0	5.1	4.3	4.3	4.5	4.3	3.9
Pb	2.3	0.7	2.4	2.9	0.6	0.4	3.2	0.5	0.4
Se	8.5	7.1	8.6	7.9	8.6	8.8	9.4	10.8	11.0
Zn	19.6	29.3	12.8	34.0	17.8	10.3	37.0	16.1	8.9
	HC								
K	1209.9	3257.1	724.3	2902.1	2208.2	1564.7	2887.5	2106.5	1427.7
Mg	318.3	1385.7	78.0	965.4	646.6	436.5	961.0	526.0	286.9
P	265.3	1828.6	300.0	1436.5	1117.1	631.4	1439.4	1101.7	866.3
As	N/A	0.1	0.1	0.1	0.1	N/A	0.1	0.1	N/A
Cd	N/A	N/A	N/A	N/A	N/A	N/A	N/A	N/A	N/A
Co	N/A	N/A	N/A	0.1	N/A	0.1	0.1	N/A	N/A
Cr	2.9	3.1	2.9	3.0	3.0	1.8	2.9	1.7	1.5
Cu	11.0	10.9	15.9	11.1	11.8	0.4	12.8	3.6	3.0
Fe	19.9	211.4	22.1	153.1	99.6	47.2	154.6	97.2	69.9
Mn	1.8	50.0	1.4	28.9	18.2	9.7	30.9	21.2	13.5
Ni	4.2	4.3	4.3	5.0	4.4	4.8	4.6	4.4	4.4
Pb	2.7	3.3	2.6	3.3	3.0	0.4	3.2	0.7	0.4
Se	12.4	11.1	13.0	11.3	11.9	10.9	12.2	11.6	12.2
Zn	14.6	44.4	13.2	34.4	24.2	9.0	38.5	26.2	16.4
	BC								
K	1703.8	3562.4	1154.3	3074.2	2840.0	2644.4	3040.0	2314.3	1717.0
Mg	112.0	869.1	6.8	510.9	569.3	398.8	704.0	431.4	256.2
P	154.5	1054.9	44.1	815.5	860.0	651.9	1038.7	754.3	471.5
As	N/A	N/A	N/A	N/A	N/A	N/A	N/A	N/A	N/A
Cd	N/A	N/A	N/A	N/A	N/A	N/A	N/A	N/A	N/A
Co	N/A	N/A	0.1	N/A	N/A	N/A	N/A	N/A	N/A
Cr	1.4	1.4	1.2	1.3	1.4	4.2	1.7	1.4	1.4
Cu	N/A	N/A	N/A	N/A	N/A	N/A	N/A	N/A	N/A
Fe	5.5	82.6	1.3	60.0	75.1	62.2	88.7	85.9	37.0
Mn	1.3	36.5	0.5	20.2	23.2	14.8	29.7	19.3	11.1
Ni	N/A	N/A	0.5	N/A	N/A	0.2	N/A	N/A	N/A
Pb	0.6	1.2	N/A	N/A	0.1	N/A	0.5	N/A	N/A
Se	8.5	8.8	7.8	8.5	8.0	8.9	8.8	8.9	8.9
Zn	2.4	20.8	N/A	13.4	18.7	13.3	48.3	14.4	12.4

As shown in Table 11, CM has the highest concentrations in K, Mg, and P across raw biomasses, hydrochars, and biochars. The CM shows consistency with the literature, where it is known to have high nutrients, especially in P and K.[139] The Mg and P decrease in biochars compare to raw biomasses and hydrochars while K increases. The decrease in concentrations was also observed in other heavy metals, where the biochars have more than 50% drop in metal concentrations. Some heavy metals such as Cd and Co were below detection limits. This was possibly due to the highly stable aromatic structures in the biochars, which decreased the extractability of K, Mg, and P even under acidic environment.[140] According to the IBI maximum allowable thresholds, all heavy metals are within the range for use as a soil amendment. To maximize the K, Mg, P, and to minimize the heavy metals that are present in the soil when using hydrochars and biochars as soil amendments, cow manure biochar is recommended due to the stable biochar structure described in the previous section. Furthermore, cow manure biochar's higher concentrations in nutrients, and lower concentrations in heavy metals are also beneficial to soil and plant growth.

4.1.10 The thermal stability of initial biomasses, hydrochars, and biochars when utilizing as soil amendments and solid fuels

To gauge the thermal stability of each sample, the derivative thermogravimetric curves are shown in Figure 12, Figure 13, and Figure 14. The DTG curves were calculated using the TG data and smoothed with 10-point moving averages from 110 ^{o}C through 910 ^{o}C. The DTG curves show the relative rates of devolatilization of the volatile matter.

Two regions are shown in the DTG curves: active pyrolysis (devolatilization region) and passive pyrolysis. In the devolatilization region in Figure 12, the corn stover and its mixtures have 30-70 % higher in the devolatilizing rate in the temperatures between 250 and 350 ^{o}C compare to cow manure and grape marc, which was an indication of the devolatilization of cellulose, hemicellulose, and partially lignin. The peaks across initial biomasses and their mixtures suggested that most devolatilization happened at around 300 ^{o}C, which shows consistency with the literature.[141] The passive pyrolysis region is shown after 375 ^{o}C, where the slow mass loss corresponds to complete devolatilization of lignin as well as char formation.[135] Furthermore, hydrochars in Figure 13 illustrated the increase in thermal stability due to the uninformative of the slopes compared to the raw biomasses. The increase in thermal stability is due to the HTC reactions at 220 ^{o}C, which converted weaker-bonded carbons into more stabilized carbons. By comparing the 2hr HC CM and 1hr HC CM, we can see that the conversion rate of 1hr HC CM was around 15% higher than the conversion rate of 2hr HC CM at 300 ^{o}C, indicating that more volatiles were converted by increasing the residence time. However, the slopes of all hydrochars (additional data in Appendix A) showed decrease devolatilizing rates, suggesting the even a slight decrease and increase in the volatile matter and fixed carbon have significant effects on thermal stabilities.[142]

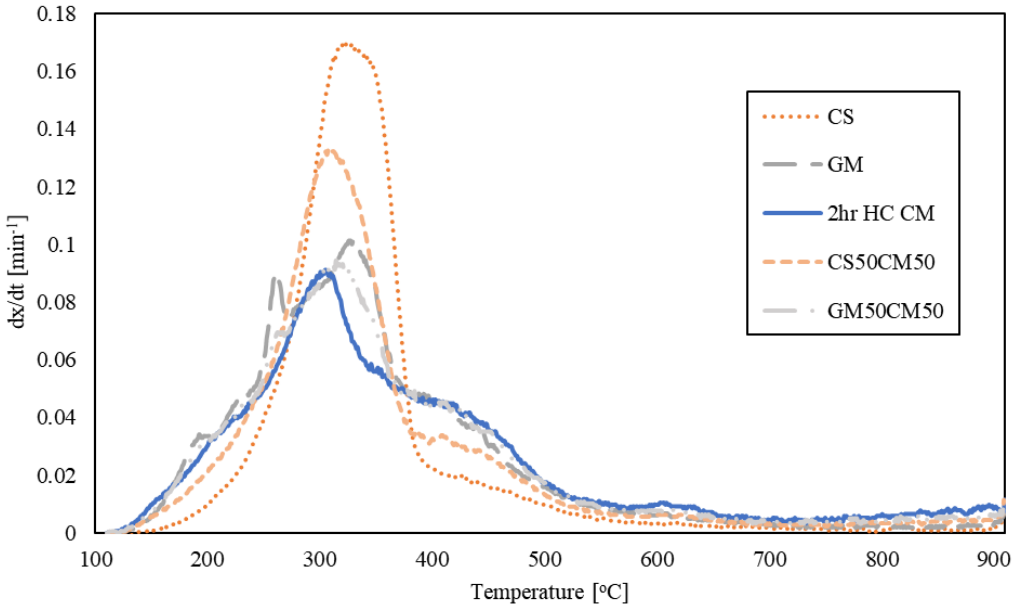

Figure 12. DTG curves of the initial biomasses and their 50:50 mixtures. More data available in Appendix A

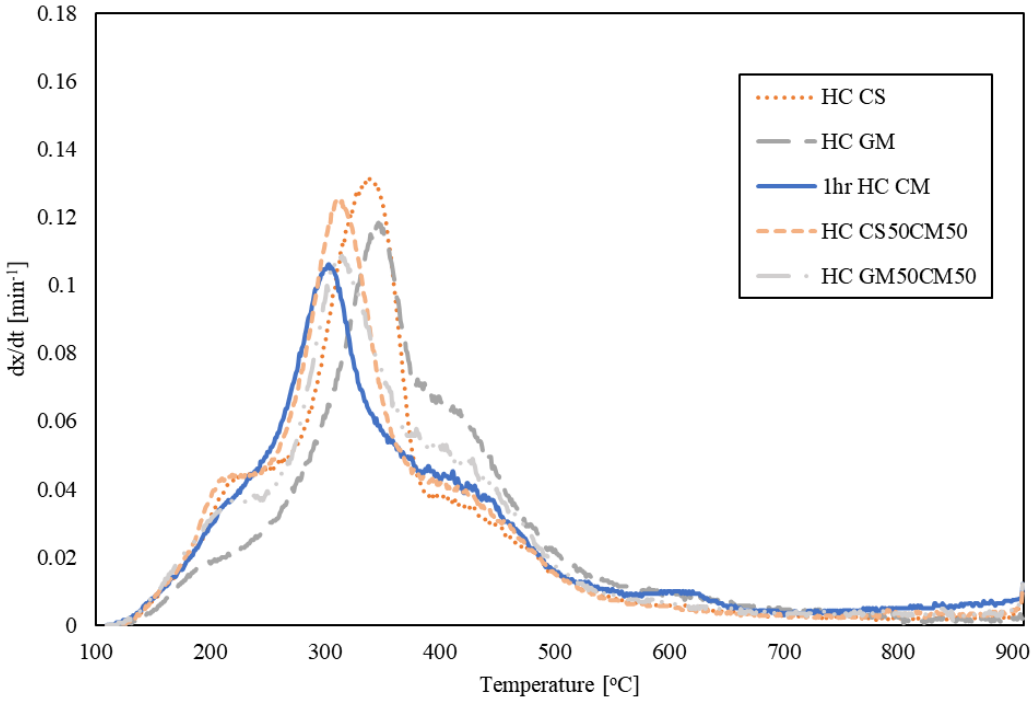

Figure 13. DTG curves of the hydrochars and their 50:50 mixtures. More data available in Appendix A

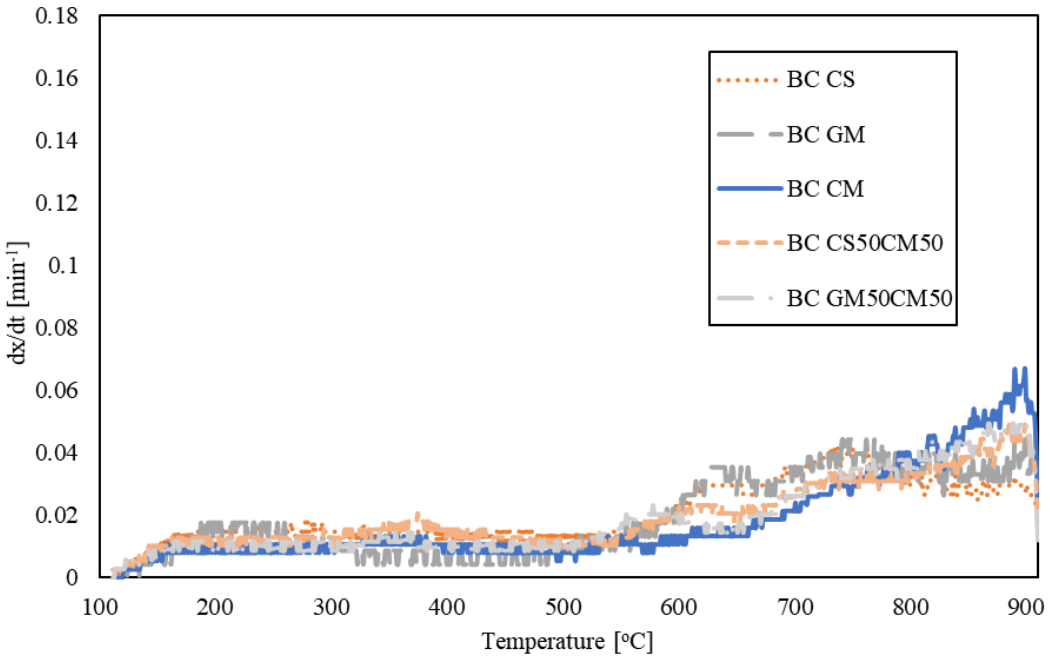

Figure 14. DTG curves of the biochars and their 50:50 mixtures. More data available in Appendix A

4.2 Fuel properties of initial biomasses, hydrochars, biochars, and bio-oil

The hydrochars and biochars could be used as soil amendments, and as solid fuels. Although coal and petroleum-based liquid fuels are known to have higher calorific values, coal and petroleum-based fuels pollutions to the environment are exacerbating global warming. By utilizing biofuels, we can reduce greenhouse gas emissions and decrease our over-reliance on fossil fuels. To determine the practicality of using hydrochars and biochars as solid fuels, we compare the heating values to such conventional fuels.

4.2.1 Hydrochars and biochars as solid fuels using Higher Heating Values

The HHV was calculated from the ultimate analysis using Dulong's Equation[143], shown in Equation 4.2.1, where C, H, N, and O are in weight percentages.

$$HHV\left[\frac{MJ}{kg}\right] = (33.5 \cdot C_{\%} + 142.3 \cdot H_{\%} - 15.4 \cdot O_{\%} - 24.5 \cdot N_{\%})/100 \qquad (4.2.1)$$

The HHVs of corn stover, cow manure, grape marc, and the mixtures are shown in Table 12. The corn stover hydrochar showed a decrease in energy content compared to its raw form - this might be due to the higher ash content in the corn stover hydrochar, which does not contribute to the heating value. In contrast, grape marc hydrochar demonstrated a significant increase in its energy density compared to its raw form, mainly due to the increase in carbon content while the ash content remains unchanged. The 1-hour and 2-hour cow manure hydrochars did not show a significant difference in HHV – this is due to the similar composition of C, H, N, O, and ash based on Equation 4.2.1. The biochars showed generally lower HHVs compared to the hydrochars and raw biomasses[144] besides grape marc. Hydrochars show higher HHVs generally compare to the initial biomasses except corn stover. The cow manure hydrochar and biochar HHVs are consistent with the literature.[145] The biochars low HHVs might be due to the limitations of Dulong's Equation using a dry basis C, H, N, O to calculate the higher heating value. Proximate analysis in the previous section suggests that biochars have approximately two times the amount of ash compare to hydrochars and raw biomasses. Since the ash mainly consists of incombustible products such as silicon oxides, it has no contribution to the heating value. Furthermore, the main contributor for the HHV is the hydrogen with the highest coefficient according to the Dulong's Equation. During pyrolysis, hydrogens in biochars were significantly reduced by 80-90% compared to the feedstocks as shown in the ultimate analysis. This can be caused by the formation of the aromatic carbons and intensified dehydration, which reduce the overall hydrogen contents.

The two most commonly used coal types are bituminous and anthracite, which have HHVs between 33-35 MJ/kg.[71] In comparison to the hydrochars and biochars, the BC GM demonstrated the closest to coals HHV value to be used as a solid fuel. Although the HHV of BC GM is 5-7 MJ/kg lower than that of bituminous coal, the biochars are a greener energy source, which significantly decreases the sulfur oxides that creates acid rain when bond to oxygen significantly. By using hydrochars upgraded from agricultural and animal waste, we could have better farm waste management and generate energy from a cleaner source.

Table 12. Calculated higher heating values of raw biomasses, hydrochars, and biochars in MJ/kg

	CS	CM	GM	CS25 CM75	CS50 CM50	CS75 CM25	GM25 CM75	GM50 CM50	GM75 CM25
Initial biomasses	23.85	20.41*	21.85	21.30	22.12	22.98	20.86	21.24	21.63
Hydrochars	21.17	19.77**	27.73	23.21	21.43	22.25	23.04	24.86	27.60
Biochars	22.42	14.63	28.03	14.01	17.93	19.70	14.66	19.89	23.05

*indicates 2hr HC CM, **indicates 1hr HC CM

4.2.2 Bio-oil analysis for potential liquid fuel produced during pyrolysis

Petroleum-based fuel is comprised of more than 90% alkanes, cycloalkanes, aromatics, and asphaltenes. Conversely, bio-oil is mainly composed of highly oxygenated compounds, with higher viscosity, acidity, and moisture content, and lower stability and calorific value.[146] Understanding the compounds in the bio-oil produced during pyrolysis is essential to explore the feasibility of utilizing bio-oil as a liquid fuel. Table 13 shows the organic compounds found in the bio-oil, which are categorized and reported under the categories of ketones, phenols, alkanes, alkenes, acids, aldehydes, alcohols, and other groups. The top 40 peaks were selected for each biomass, which were matched to the mass spectrometry library (NIST) for compounds

with a minimum similarity of 80%. More detailed compounds of each group are also available in Appendix B.

As seen in Table 13, the oil produced by corn stover has significantly more ketones, followed by the grape marc and the cow manure. The oil produced from the cow manure mainly consists of phenols, alkanes, and acids, which add up to more than 80% (by area). The cow manure bio-oil contained longer saturated alkane chains and acids that appeared later in the gas chromatograph with the most significant peak at around 101 min (Methyl Stearate). This peak was exclusive to cow manure as it only appeared in the cow manure and its mixtures. Methyl Stearate is a saturated methyl ester and is a key molecule in the biofuel which comes from the fatty acids from vegetables and animal fats.[147] This explained why the cow manure bio-oil had methyl stearate in it. The oil produced from grape marc was around 54% (by area) phenols, with 11% - 12% (by area) of ketones and alkanes. Furthermore, either trace or no alkanes, alkenes, and acids were registered to the top 40 peaks in corn stover bio-oil; Either trace or no aldehydes and alcohols were registered to the top 40 peaks in cow manure bio-oil. Since all compounds besides alkanes and alkenes have at least one oxygen attached to the group, it makes the bio-oil acidic, viscous, and unstable. Unstable bio-oil degrades over time and causes severe problems such as corrosion and poor efficiency on conventional gas turbines.[148] The oxygenated compounds (ketones, phenols, aldehydes, alcohols) and water in the bio-oil are the causes for the low calorific value (~1/3 compare to petroleum-based fuel).[146] The phenolic compounds and acids lower the pH of the bio-oil, making it more corrosive and accelerate its degradation.[149]

Synergistic effects were also seen in Table 13 (bolded) in the mixtures. By mixing corn stover with the cow manure, phenols increased by an average of 6% compared to the bio-oils produced from corn stover or cow manure. The GM25CM75 mixture promoted the formation of alkanes and alkenes by an average of 15% and 5%, respectively. The GM75CM25 mixture enhanced the ketones and phenols formation by 5% and 2%, respectively. The formation of alkanes and alkenes are beneficial for liquid fuels as they are saturated carbons that stabilize the bio-oil and decrease the water content and viscosity. The formation of oxygenated compounds such as ketones and phenols have negative effects on the fuel characteristics as they are prone to acidify the fuel and make the fuel unstable. The reduced intensities in the biochar FTIR spectra could be compensated by the compounds in the oil produced from the pyrolysis feed, as most of the organic matter devolatilized during pyrolysis to form bio-oil or in the exiting gas. The differences in the biochar and feed agreed with the enhancement of the compounds listed in Table 13, suggesting that temperature, along with the mixing of lignocellulosic biomasses and cow manure, has synergistic effects during the pyrolysis process that lead to the increase in more phenolic groups in CS-CM mixtures and more alkanes/alkenes in GM25CM75.

Table 13. Organic compounds in bio-oils produced during pyrolysis by groups in area percentages

	CS	CM	GM	CS25 CM75	CS50 CM50	CS75 CM25	GM25 CM75	GM50 CM50	GM75 CM25
Ketones	40.09	5.36	11.46	15.03	27.11	33.50	7.34	9.57	**13.98**
Phenols	28.18	30.47	54.48	**33.58**	**34.03**	**38.20**	28.73	40.88	46.91
Alkanes	0.00	30.94	11.86	25.37	9.60	2.03	**36.69**	21.95	11.77
Alkenes	0.00	5.75	0.72	1.95	0.00	0.00	**7.88**	3.40	2.10
Aldehydes	9.85	0.00	9.42	0.00	3.25	5.49	0.00	2.32	5.49
Alcohols	13.73	0.00	1.93	3.28	9.63	11.00	1.78	1.95	**4.48**
Acids	0.00	22.78	2.94	15.97	9.74	4.64	13.38	15.47	7.75
Others	8.15	4.71	7.19	4.82	6.63	5.13	4.21	4.46	7.51

Chapter 5: Conclusion

This work explores the optimal pathway to produce nutrient-enriched soil amendments and biofuel from dry agricultural and animal waste. HTC/co-HTC and pyrolysis/co-pyrolysis were performed on corn stover, grape marc, cow manure, and their mixtures to produce hydrochars and biochars. A combined HTC-pyrolysis process was investigated to convert farm waste to usable soil amendments and biofuels, producing higher nutrient and surface area biochars. The H/C ratios of raw biomasses and hydrochars are similar (1.0-1.2), but the hydrochars have a lower O/C ratio, suggesting that more oxygens were driven off during the HTC process, mainly from decarboxylation and dehydration. Biochars have the lowest H/C and O/C ratios compare the hydrochars and raw biomasses, indicating high stability, which is good for resisting degradation and microbial activities. All biochars are basic, while raw grape marc and all other hydrochars are acidic, due to the highly oxygenated and hydrogenated compounds in the hydrochars. This allows biochar to be used as buffers to neutralize acidic soil. The biochars showed relatively higher surface areas than the hydrochars and raw biomasses apart from grape marc. The overall amount of surface functional groups of biochars decreased across the wavenumbers, which was explained by the pyrolysis process that intensified dehydration, driving off more oxygen and hydrogens, hence resulting in higher C=C and C-H aromatics and fewer C-H aliphatic, C-O, and O-H compounds. The development of aromatic compounds stabilizes biochars, which makes them a better choice for soil amendments. The 1hr HC cow manure has the most bioavailable Mg and P while the BC cow manure has the most K. Hydrochars also have slightly higher bioavailable heavy metals

concentrations compared to raw biomasses and biochars. The biochars show overall lower in bioavailable nutrient and heavy metals concentrations compared to hydrochars and raw biomasses, most likely due to the stable carbon structure developed in the biochars, which increased the difficulty of nutrient leaching. All nutrients measured are within the IBI maximum allowable threshold. The biochars illustrate the highest thermal stability in the temperature between 110 – 910 ^{o}C, followed by the hydrochars and raw biomasses, making biochars feasible soil amendments due to their high stability. BC GM showed the highest HHV, which is also the closest to the HHVs of bituminous and anthracite coals. Even though the HHVs of biochars are lower than conventional fossil fuels (i.e., bituminous and anthracite coals), the reduction in sulfur and greenhouse gas emission is beneficial to the environment. The pyrolysis bio-oil from cow manure is most suitable to serve as a liquid fuel precursor due to its higher alkane, alkene, and lower oxygen-contained groups. Synergistic effects were seen in the production of bio-oils, where the alkanes and alkenes were promoted in the GM25CM75 bio-oil; ketones and phenols were promoted in the GM75CM25 bio-oil. When mixing corn stover with 2hr HC CM, phenolic groups were promoted. While there are still significant amounts of oxygenated compounds in the bio-oil, upgrading methods such as hydrodeoxygenation can turn phenolic groups into alkenes and alkanes. Therefore, based on the organic compounds analyzed, the GM25CM75 bio-oil is recommended for the utilization as the liquid fuel source.

Lastly, biochars overall are a better soil amendment than hydrochars, shown in Table 14, due to their possessive to stabilize soil to reduce effects from environmental

fluctuations, neutralize acidic soil for maximizing productivity, and higher surface area for water and nutrient retention. However, the hydrochars are enriched in bio-available nutrients, making them a better nutrient source than biochars. By integrating hydrocarbonized cow manure with dried agricultural waste, we found that the concentrations of the nutrients (P, Mg, K) in biochars did increase. The data suggest that pyrolyzing carbonized biomass (cow manure) results in high surface area, possibly due to the structural carbons formed during the HTC process. If considered replacing the conventional fertilizers with biochars to improve soil properties, and use the hydrochars from HTC and bio-oil from pyrolysis as energy sources, we can mitigate the environmental impacts from the chemical fertilizers and greenhouse gas emissions, hence, leading to a better farm waste management and providing energy sustainably.

Table 14. Properties of amendments that affect soil properties. (+ indicates better, 0 indicates neutral, and – indicates worse)

Characteristics	Raw	Hydrochars	Biochars
Fixed carbon	-	0	+
Stability	-	0	+
pH	Acidic	Acidic	Basic
EC	0	-	+
Hydroxyl functionalities	0	+	-
Surface area	-	0	+
Bioavailable Nutrients	0	+	-
Bioavailable heavy metals	0	+	-
Thermal stability	-	0	+
Solid fuel (HHVs)	0	-	+

References

(1) Harris, W. G.; Wilkie, A. C.; Cao, X.; Sirengo, R. Bench-Scale Recovery of Phosphorus from Flushed Dairy Manure Wastewater. *Bioresour. Technol.* **2008**, *99* (8), 3036–3043. https://doi.org/10.1016/j.biortech.2007.06.065.

(2) Camargo, G. G. T.; Ryan, M. R.; Richard, T. L. Energy Use and Greenhouse Gas Emissions from Crop Production Using the Farm Energy Analysis Tool. *Bioscience* **2013**, *63* (4), 263–273. https://doi.org/10.1525/bio.2013.63.4.6.

(3) Koneswaran, G.; Nierenberg, D.; Farm, G.; Production, A.; Change, M. C. Global Farm Animal Production and Global Warming : Impacting and Mitigating Climate Change. *Environ. Health Perspect.* **2008**, *116* (5), 578–582. https://doi.org/10.1289/ehp.ll034.

(4) Gascó, G.; Paz-Ferreiro, J.; Álvarez, M. L.; Saa, A.; Méndez, A. Biochars and Hydrochars Prepared by Pyrolysis and Hydrothermal Carbonisation of Pig Manure. *Waste Manag.* **2018**, *79*, 395–403. https://doi.org/10.1016/j.wasman.2018.08.015.

(5) Ghanim, B. M.; Pandey, D. S.; Kwapinski, W.; Leahy, J. J. Hydrothermal Carbonisation of Poultry Litter: Effects of Treatment Temperature and Residence Time on Yields and Chemical Properties of Hydrochars. *Bioresour. Technol.* **2016**, *216*, 373–380. https://doi.org/10.1016/j.biortech.2016.05.087.

(6) Volpe, M.; Goldfarb, J. L.; Fiori, L. Hydrothermal Carbonization of Opuntia Ficus-Indica Cladodes: Role of Process Parameters on Hydrochar Properties. *Bioresour. Technol.* **2018**, *247*, 310–318. https://doi.org/10.1016/j.biortech.2017.09.072.

(7) Piro, G.; Fiori, L.; Lucian, M.; Volpe, M.; Gao, L.; Goldfarb, J. L. Impact of Hydrothermal Carbonization Conditions on the Formation of Hydrochars and Secondary Chars from the Organic Fraction of Municipal Solid Waste. *Fuel* **2018**, *233* (January), 257–268. https://doi.org/10.1016/j.fuel.2018.06.060.

(8) Zornoza, R.; Moreno-Barriga, F.; Acosta, J. A.; Muñoz, M. A.; Faz, A. Stability, Nutrient Availability and Hydrophobicity of Biochars Derived from Manure, Crop Residues, and Municipal Solid Waste for Their Use as Soil Amendments. *Chemosphere* **2016**, *144*, 122–130. https://doi.org/10.1016/j.chemosphere.2015.08.046.

(9) Libra, J. A.; Ro, K. S.; Kammann, C.; Funke, A.; Berge, N. D.; Neubauer, Y.; Titirici, M.-M.; Fühner, C.; Bens, O.; Kern, J.; et al. Hydrothermal Carbonization of Biomass Residuals: A Comparative Review of the Chemistry, Processes and Applications of Wet and Dry Pyrolysis. *Biofuels* **2011**, *2* (1), 71–106. https://doi.org/10.4155/bfs.10.81.

(10) Rosegrant, M.; Cai, X.; Cline, S. *World Water and Food to 2025*; 2002. https://doi.org/0-89629-646-6.

(11) Smil, V. Nitrogen in Crop Production: An Account of Global Flows. *Global Biogeochem. Cycles* **1999**, *13* (2), 647–662. https://doi.org/10.1029/1999GB900015.

(12) Wood, S.; Scherr, S. J. *Pilot Analysis of Global Ecosystems: Agroecosystems*; World Resources Institute, 2000.

(13) USDOE. *U.S. Billion-Ton Update: Crop Residues and Agricultural Wastes*; 2011.
(14) Cuéllar, A. D.; Webber, M. E. Cow Power: The Energy and Emissions Benefits of Converting Manure to Biogas. *Environ. Res. Lett.* **2008**, *3* (3). https://doi.org/10.1088/1748-9326/3/3/034002.
(15) Heidenreich, S.; Müller, M.; Foscolo, P. U. Biomass Pretreatment. *Adv. Biomass Gasif.* **2016**, 11–17. https://doi.org/10.1016/b978-0-12-804296-0.00003-8.
(16) Ciuta, S.; Tsiamis, D.; Castaldi, M. J. Fundamentals of Gasification and Pyrolysis. In *Gasification of Waste Materials*; 2018; pp 13–36. https://doi.org/10.1016/b978-0-12-812716-2.00002-9.
(17) Nunes, L. J. R.; De Oliveira Matias, J. C.; Da Silva Catalão, J. P. Introduction. In *Torrefaction of Biomass for Energy Applications*; 2018; pp 1–43. https://doi.org/10.1016/b978-0-12-809462-4.00001-8.
(18) Kumar, S.; Ankaram, S. *Waste-to-Energy Model/Tool Presentation*; Elsevier B.V., 2019. https://doi.org/10.1016/b978-0-444-64083-3.00012-9.
(19) Kumar, S.; Ankaram, S. *Waste-to-Energy Model/Tool Presentation*; Elsevier B.V., 2019. https://doi.org/10.1016/b978-0-444-64083-3.00012-9.
(20) Biller, P.; Ross, A. B. *Production of Biofuels via Hydrothermal Conversion*; Elsevier Ltd, 2016. https://doi.org/10.1016/B978-0-08-100455-5.00017-5.
(21) Baronti, S.; Alberti, G.; Camin, F.; Criscuoli, I.; Genesio, L.; Mass, R.; Vaccari, F. P.; Ziller, L.; Miglietta, F. Hydrochar Enhances Growth of Poplar for Bioenergy While Marginally Contributing to Direct Soil Carbon Sequestration. *GCB Bioenergy* **2017**, *9* (11), 1618–1626. https://doi.org/10.1111/gcbb.12450.
(22) Mašek, O. Biochar in Thermal and Thermochemical Biorefineries-Production of Biochar as a Coproduct. *Handb. Biofuels Prod. Process. Technol. Second Ed.* **2016**, 655–671. https://doi.org/10.1016/B978-0-08-100455-5.00021-7.
(23) Cai, J.; Li, B.; Chen, C.; Wang, J.; Zhao, M.; Zhang, K. Hydrothermal Carbonization of Tobacco Stalk for Fuel Application. *Bioresour. Technol.* **2016**, *220*, 305–311. https://doi.org/10.1016/j.biortech.2016.08.098.
(24) Ruan, R.; Zhang, Y.; Chen, P.; Liu, S.; Fan, L.; Zhou, N.; Ding, K.; Peng, P.; Addy, M.; Cheng, Y.; et al. *Biofuels: Alternative Feedstocks and Conversion Processes for the Production of Liquid and Gaseous Biofuels (Second Edition)*; 2019. https://doi.org/10.1016/b978-0-12-816856-1.00001-4.
(25) Kambo Harpreet Singh, D. A. A Comparative Review of Biochar and Hydrochar in Terms of Production, Physico-Chemical Properties and Applications. *Renew. Sustain. Energy Rev.* **2015**, *45*, 359–378. https://doi.org/10.1016/j.rser.2015.01.050.
(26) Deem, L. M.; Crow, S. E. Biochar. *Ref. Modul. Earth Syst. Environ. Sci.* **2017**, 1–5. https://doi.org/10.1016/b978-0-12-409548-9.10524-x.
(27) Itskos, G.; Nikolopoulos, N.; Kourkoumpas, D. S.; Koutsianos, A.; Violidakis, I.; Drosatos, P.; Grammelis, P. *Energy and the Environment*; Elsevier B.V., 2016. https://doi.org/10.1016/B978-0-444-62733-9.00006-X.
(28) Roddy, D. J.; Manson-Whitton, C. *Biomass Gasification and Pyrolysis*; Elsevier Ltd., 2012; Vol. 5. https://doi.org/10.1016/B978-0-08-087872-

0.00514-X.
(29) Jakab, E. *Analytical Techniques as a Tool to Understand the Reaction Mechanism*; Elsevier B.V., 2015. https://doi.org/10.1016/B978-0-444-63289-0.00003-X.
(30) Zaman, C. Z.; Pal, K.; Yehye, W. A.; Sagadevan, S.; Shah, S. T.; Adebisi, G. A.; Marliana, E.; Rafique, R. F.; Johan, R. Bin. Pyrolysis: A Sustainable Way to Generate Energy from Waste. *Pyrolysis* **2017**, 3–36. https://doi.org/10.5772/intechopen.69036.
(31) Reza Nemati, M.; Simard, F.; Fortin, J. P.; Beaudoin, J. Potential Use of Biochar in Growing Media. *Vadose Zo. J.* **2015**, *14* (6), 1–8. https://doi.org/10.2136/vzj2014.06.0074.
(32) DING, Y.; LIU, Y.; LIU, S.; HUANG, X.; LI, Z.; TAN, X.; ZENG, G.; ZHOU, L. Potential Benefits of Biochar in Agricultural Soils: A Review. *Pedosphere* **2017**, *27* (4), 645–661. https://doi.org/10.1016/S1002-0160(17)60375-8.
(33) Zhao, J. J.; Shen, X. J.; Domene, X.; Alcañiz, J. M.; Liao, X.; Palet, C. Comparison of Biochars Derived from Different Types of Feedstock and Their Potential for Heavy Metal Removal in Multiple-Metal Solutions. *Sci. Rep.* **2019**, *9* (1), 1–12. https://doi.org/10.1038/s41598-019-46234-4.
(34) Rawat, J.; Saxena, J.; Sanwal, P. Biochar: A Sustainable Approach for Improving Plant Growth and Soil Properties. *Biochar - An Imp. Amend. Soil Environ.* **2019**. https://doi.org/10.5772/intechopen.82151.
(35) Ralebitso-Senior, T. K.; Orr, C. H. *Microbial Ecology Analysis of Biochar-Augmented Soils: Setting the Scene*; Elsevier Inc., 2016. https://doi.org/10.1016/B978-0-12-803433-0.00001-1.
(36) Cordell, D.; Drangert, J. O.; White, S. The Story of Phosphorus: Global Food Security and Food for Thought. *Glob. Environ. Chang.* **2009**, *19* (2), 292–305. https://doi.org/10.1016/j.gloenvcha.2008.10.009.
(37) Takaya, C. A.; Parmar, K. R.; Fletcher, L. A.; Ross, A. B. Biomass-Derived Carbonaceous Adsorbents for Trapping Ammonia. *Agric.* **2019**, *9* (1). https://doi.org/10.3390/agriculture9010016.
(38) Ketterings, Q. M.; Albrecht, G.; Beckman, J. Soil PH for Field Crops: Agronomy Fact Sheet Series. **2005**, 2.
(39) Horrocks, R. D.; Vallentine, J. F. Soil Fertility and Forage Production. *Harvest. Forages* **1999**, 187–224. https://doi.org/10.1016/b978-012356255-5/50033-x.
(40) Baghdadi, A.; Halim, R. A.; Ghasemzadeh, A.; Ramlan, M. F.; Sakimin, S. Z. Impact of Organic and Inorganic Fertilizers on the Yield and Quality of Silage Corn Intercropped with Soybean. *PeerJ* **2018**, *2018* (10). https://doi.org/10.7717/peerj.5280.
(41) Hyland, C.; Ketterings, Q.; Dewing, D.; Stockin, K.; Czymmek, K.; Albrecht, G.; Geohring, L. *The Phosphorus Cycle - Agronomy Factsheet*; 2005. https://doi.org/10.1016/S0065-2881(05)48011-6.
(42) Attfield, J. P. Phosphates. In *Encyclopedia of Materials: Science and Technology (Second Edition)*; 2001; pp 6896–6901. https://doi.org/https://doi.org/10.1016/B0-08-043152-6/01222-5.
(43) Guoqin, H. The Role of Potassium in Plants under Drought Stress: Mini

Review. *J. Basic Appl. Sci.* **2017**, *13*, 268–271. https://doi.org/10.6000/1927-5129.2017.13.44.
(44) Prajapati, K.; Modi, H. A. The Importance of Potassium in Plant Growth – a Review. *Indian J. Plant Sci. Jul.-Sept. Oct.-Dec* **2012**, *1* (June), 2319–382402.
(45) WANG, L.; DUAN, G. Effect of External and Internal Phosphate Status on Arsenic Toxicity and Accumulation in Rice Seedlings. *J. Environ. Sci.* **2009**, *21* (3), 346–351. https://doi.org/10.1016/S1001-0742(08)62275-5.
(46) Yousaf, M.; Li, J.; Lu, J.; Ren, T.; Cong, R.; Fahad, S.; Li, X. Effects of Fertilization on Crop Production and Nutrient-Supplying Capacity under Rice-Oilseed Rape Rotation System. *Sci. Rep.* **2017**, *7* (1), 1–9. https://doi.org/10.1038/s41598-017-01412-0.
(47) Saha, N.; Saba, A.; Reza, M. T. Effect of Hydrothermal Carbonization Temperature on PH, Dissociation Constants, and Acidic Functional Groups on Hydrochar from Cellulose and Wood. *J. Anal. Appl. Pyrolysis* **2019**, *137* (November 2018), 138–145. https://doi.org/10.1016/j.jaap.2018.11.018.
(48) Kalderis, D.; Kotti, M. S.; Méndez, A.; Gascó, G. Characterization of Hydrochars Produced by Hydrothermal Carbonization of Rice Husk. *Solid Earth* **2014**, *5* (1), 477–483. https://doi.org/10.5194/se-5-477-2014.
(49) Wang, T.; Zhai, Y.; Zhu, Y.; Li, C.; Zeng, G. A Review of the Hydrothermal Carbonization of Biomass Waste for Hydrochar Formation: Process Conditions, Fundamentals, and Physicochemical Properties. *Renew. Sustain. Energy Rev.* **2018**, *90* (February), 223–247. https://doi.org/10.1016/j.rser.2018.03.071.
(50) Antero, R. V. P.; Alves, A. C. F.; de Oliveira, S. B.; Ojala, S. A.; Brum, S. S. Challenges and Alternatives for the Adequacy of Hydrothermal Carbonization of Lignocellulosic Biomass in Cleaner Production Systems: A Review. *J. Clean. Prod.* **2020**, *252*, 119899. https://doi.org/10.1016/j.jclepro.2019.119899.
(51) Bargmann, I.; Rillig, M. C.; Kruse, A.; Greef, J. M.; Kücke, M. Effects of Hydrochar Application on the Dynamics of Soluble Nitrogen in Soils and on Plant Availability. *J. Plant Nutr. Soil Sci.* **2014**, *177* (1), 48–58. https://doi.org/10.1002/jpln.201300069.
(52) Xia, Y.; Liu, H.; Guo, Y.; Liu, Z.; Jiao, W. Immobilization of Heavy Metals in Contaminated Soils by Modified Hydrochar: Efficiency, Risk Assessment and Potential Mechanisms. *Sci. Total Environ.* **2019**, *685*, 1201–1208. https://doi.org/10.1016/j.scitotenv.2019.06.288.
(53) Biederman, L. A.; Stanley Harpole, W. Biochar and Its Effects on Plant Productivity and Nutrient Cycling: A Meta-Analysis. *GCB Bioenergy* **2013**, *5* (2), 202–214. https://doi.org/10.1111/gcbb.12037.
(54) Guo, X. xia; Liu, H. tao; Zhang, J. The Role of Biochar in Organic Waste Composting and Soil Improvement: A Review. *Waste Manag.* **2020**, *102*, 884–899. https://doi.org/10.1016/j.wasman.2019.12.003.
(55) Aziz, N. S. binti A.; Nor, M. A. bin M.; Manaf, S. F. binti A.; Hamzah, F. Suitability of Biochar Produced from Biomass Waste as Soil Amendment. *Procedia - Soc. Behav. Sci.* **2015**, *195*, 2457–2465. https://doi.org/10.1016/j.sbspro.2015.06.288.
(56) Wu, Z.; Zhang, X.; Dong, Y.; Li, B.; Xiong, Z. Biochar Amendment Reduced

Greenhouse Gas Intensities in the Rice-Wheat Rotation System: Six-Year Field Observation and Meta-Analysis. *Agric. For. Meteorol.* **2019**, *278* (January). https://doi.org/10.1016/j.agrformet.2019.107625.

(57) Mandal, S.; Donner, E.; Smith, E.; Sarkar, B.; Lombi, E. Biochar with Near-Neutral PH Reduces Ammonia Volatilization and Improves Plant Growth in a Soil-Plant System: A Closed Chamber Experiment. *Sci. Total Environ.* **2019**, *697*, 134114. https://doi.org/10.1016/j.scitotenv.2019.134114.

(58) Lehmann, J.; Rillig, M. C.; Thies, J.; Masiello, C. A.; Hockaday, W. C.; Crowley, D. Biochar Effects on Soil Biota - A Review. *Soil Biol. Biochem.* **2011**, *43* (9), 1812–1836. https://doi.org/10.1016/j.soilbio.2011.04.022.

(59) Lehmann, J.; Rillig, M. C.; Thies, J.; Masiello, C. A.; Hockaday, W. C.; Crowley, D. Biochar Effects on Soil Biota - A Review. *Soil Biol. Biochem.* **2011**, *43* (9), 1812–1836. https://doi.org/10.1016/j.soilbio.2011.04.022.

(60) Zhang, S.; Zhu, X.; Zhou, S.; Shang, H.; Luo, J.; Tsang, D. C. W. *Hydrothermal Carbonization for Hydrochar Production and Its Application*; Elsevier Inc., 2019. https://doi.org/10.1016/b978-0-12-811729-3.00015-7.

(61) Zhou, S.; Liang, H.; Han, L.; Huang, G.; Yang, Z. The Influence of Manure Feedstock, Slow Pyrolysis, and Hydrothermal Temperature on Manure Thermochemical and Combustion Properties. *Waste Manag.* **2019**, *88*, 85–95. https://doi.org/10.1016/j.wasman.2019.03.025.

(62) Speight, J. G. *Properties of Organic Compounds*; 2017. https://doi.org/10.1016/b978-0-12-804492-6.00005-8.

(63) Stauffer, E.; Dolan, J. A.; Newman, R. Review of Basic Organic Chemistry. *Fire Debris Anal.* **2008**, 49–83. https://doi.org/10.1016/b978-012663971-1.50007-5.

(64) Wu, Q.; Xian, Y.; He, Z.; Zhang, Q.; Wu, J.; Yang, G.; Zhang, X.; Qi, H.; Ma, J.; Xiao, Y.; et al. Adsorption Characteristics of Pb(II) Using Biochar Derived from Spent Mushroom Substrate. *Sci. Rep.* **2019**, *9* (1), 1–11. https://doi.org/10.1038/s41598-019-52554-2.

(65) Fagern, L. Formation and Behaviour of Organic Compounds in Biomass Dryers. **1993**, *46*, 71–76.

(66) Zhao, S. X.; Ta, N.; Wang, X. D. Effect of Temperature on the Structural and Physicochemical Properties of Biochar with Apple Tree Branches as Feedstock Material. *Energies* **2017**, *10* (9). https://doi.org/10.3390/en10091293.

(67) Qambrani, N. A.; Rahman, M. M.; Won, S.; Shim, S.; Ra, C. Biochar Properties and Eco-Friendly Applications for Climate Change Mitigation, Waste Management, and Wastewater Treatment: A Review. *Renew. Sustain. Energy Rev.* **2017**, *79* (November 2016), 255–273. https://doi.org/10.1016/j.rser.2017.05.057.

(68) Jian, X.; Zhuang, X.; Li, B.; Xu, X.; Wei, Z.; Song, Y.; Jiang, E. Comparison of Characterization and Adsorption of Biochars Produced from Hydrothermal Carbonization and Pyrolysis. *Environ. Technol. Innov.* **2018**, *10*, 27–35. https://doi.org/10.1016/j.eti.2018.01.004.

(69) Fu, M. M.; Mo, C. H.; Li, H.; Zhang, Y. N.; Huang, W. X.; Wong, M. H. Comparison of Physicochemical Properties of Biochars and Hydrochars

Produced from Food Wastes. *J. Clean. Prod.* **2019**, *236*, 117637. https://doi.org/10.1016/j.jclepro.2019.117637.
(70) Dashti, A.; Noushabadi, A. S.; Raji, M.; Razmi, A.; Ceylan, S.; Mohammadi, A. H. Estimation of Biomass Higher Heating Value (HHV) Based on the Proximate Analysis: Smart Modeling and Correlation. *Fuel* **2019**, *257* (August), 115931. https://doi.org/10.1016/j.fuel.2019.115931.
(71) Carvill, J. Thermodynamics and Heat Transfer. In *Mechanical Engineer's Data Handbook*; 1993; Vol. 1. https://doi.org/10.1016/B978-0-08-051135-1.50008-X.
(72) Boumanchar, I.; Chhiti, Y.; M'hamdi Alaoui, F. E.; El Ouinani, A.; Sahibed-Dine, A.; Bentiss, F.; Jama, C.; Bensitel, M. Effect of Materials Mixture on the Higher Heating Value: Case of Biomass, Biochar and Municipal Solid Waste. *Waste Manag.* **2017**, *61*, 78–86. https://doi.org/10.1016/j.wasman.2016.11.012.
(73) Crombie, K.; Mašek, O. Pyrolysis Biochar Systems, Balance between Bioenergy and Carbon Sequestration. *GCB Bioenergy* **2015**, *7* (2), 349–361. https://doi.org/10.1111/gcbb.12137.
(74) Ronsse, F.; van Hecke, S.; Dickinson, D.; Prins, W. Production and Characterization of Slow Pyrolysis Biochar: Influence of Feedstock Type and Pyrolysis Conditions. *GCB Bioenergy* **2013**, *5* (2), 104–115. https://doi.org/10.1111/gcbb.12018.
(75) Basu, P. *Biomass Characteristics*, First Edit.; © 2010 Elsevier Inc., 2010. https://doi.org/10.1016/b978-0-12-374988-8.00002-7.
(76) Peters, K. E.; Xia, X.; Pomerantz, A. E.; Mullins, O. C. *Geochemistry Applied to Evaluation of Unconventional Resources*; 2016. https://doi.org/10.1016/B978-0-12-802238-2.00003-1.
(77) Xing, J.; Luo, K.; Wang, H.; Gao, Z.; Fan, J. A Comprehensive Study on Estimating Higher Heating Value of Biomass from Proximate and Ultimate Analysis with Machine Learning Approaches. *Energy* **2019**, *188*, 116077. https://doi.org/10.1016/j.energy.2019.116077.
(78) Qi, J.; Zhao, J.; Xu, Y.; Wang, Y.; Han, K. Segmented Heating Carbonization of Biomass: Yields, Property and Estimation of Heating Value of Chars. *Energy* **2018**, *144*, 301–311. https://doi.org/10.1016/j.energy.2017.12.036.
(79) Basso, D.; Patuzzi, F.; Castello, D.; Baratieri, M.; Rada, E. C.; Weiss-Hortala, E.; Fiori, L. Agro-Industrial Waste to Solid Biofuel through Hydrothermal Carbonization. *Waste Manag.* **2016**, *47*, 114–121. https://doi.org/10.1016/j.wasman.2015.05.013.
(80) Pariyar, P.; Kumari, K.; Kumar, M.; Jadhao, P. S. Evaluation of Change in Biochar Properties Derived from Different Feedstock and Pyrolysis Temperature for Environmental and Agricultural Application. *Sci. Total Environ.* **2020**, *713*, 136433. https://doi.org/10.1016/j.scitotenv.2019.136433.
(81) Zhou, S.; Liang, H.; Han, L.; Huang, G.; Yang, Z. The Influence of Manure Feedstock, Slow Pyrolysis, and Hydrothermal Temperature on Manure Thermochemical and Combustion Properties. *Waste Manag.* **2019**, *88*, 85–95. https://doi.org/10.1016/j.wasman.2019.03.025.
(82) Lyu, G.; Wu, S.; Zhang, H. Estimation and Comparison of Bio-Oil Components

from Different Pyrolysis Conditions. *Front. Energy Res.* **2015**, *3* (JUN), 1–11. https://doi.org/10.3389/fenrg.2015.00028.
(83) Basu, P. *Production of Synthetic Fuels and Chemicals from Biomass*, First Edit.; © 2010 Elsevier Inc., 2010. https://doi.org/10.1016/b978-0-12-374988-8.00009-x.
(84) Cordella, M.; Torri, C.; Adamiano, A.; Fabbri, D.; Barontini, F.; Cozzani, V. Bio-Oils from Biomass Slow Pyrolysis: A Chemical and Toxicological Screening. *J. Hazard. Mater.* **2012**, *231–232*, 26–35. https://doi.org/10.1016/j.jhazmat.2012.06.030.
(85) Czernik, S.; Bridgwater, A. V. Overview of Applications of Biomass Fast Pyrolysis Oil. *Energy and Fuels* **2004**, *18* (2), 590–598. https://doi.org/10.1021/ef034067u.
(86) Chen, T.; Liu, R.; Scott, N. R. Characterization of Energy Carriers Obtained from the Pyrolysis of White Ash, Switchgrass and Corn Stover - Biochar, Syngas and Bio-Oil. *Fuel Process. Technol.* **2016**, *142*, 124–134. https://doi.org/10.1016/j.fuproc.2015.09.034.
(87) Dawodu, F. A.; Ayodele, O. O.; Akintola, J. O.; Obembe, O. A.; Sanni, A. O.; Agbejinmi, B. D. Upgrading Bio-Oil Produced from Corn Cobs and Cedrela Odorata via Catalytic Olefination and Esterification with 3,7-Dimethyloct-1-Ene and Butanol. *Int. J. Chem. Eng.* **2019**, *2019*. https://doi.org/10.1155/2019/9042425.
(88) Volpe, M.; Goldfarb, J. L.; Fiori, L. Hydrothermal Carbonization of Opuntia Ficus-Indica Cladodes: Role of Process Parameters on Hydrochar Properties. *Bioresour. Technol.* **2018**, *247* (June), 310–318. https://doi.org/10.1016/j.biortech.2017.09.072.
(89) Fiori, L.; Basso, D.; Castello, D.; Baratieri, M. Hydrothermal Carbonization of Biomass: Design of a Batch Reactor and Preliminary Experimental Results. *Chem. Eng. Trans.* **2014**, *37*, 55–60. https://doi.org/10.3303/CET1437010.
(90) Volpe, M.; Goldfarb, J. L.; Fiori, L. Hydrothermal Carbonization of Opuntia Ficus-Indica Cladodes: Role of Process Parameters on Hydrochar Properties. *Bioresour. Technol.* **2018**, *247* (September 2017), 310–318. https://doi.org/10.1016/j.biortech.2017.09.072.
(91) Bharadwaj, A.; Baxter, L. L.; Robinson, A. L. Effects of Intraparticle Heat and Mass Transfer on Biomass Devolatilization: Experimental Results and Model Predictions. *Energy and Fuels* **2004**, *18* (4), 1021–1031. https://doi.org/10.1021/ef0340357.
(92) Practice, S. Standard Practice for Proximate Analysis of Coal and Coke 1. *Annu. B. ASTM Stand.* **2013**, 3174–3175. https://doi.org/10.1520/D3172-13.2.
(93) ASTM. D3173/D3173M Standard Test Method for Moisture in the Analysis Sample of Coal and Coke. *ASTM Int.* **2011**, *i*, 7–9. https://doi.org/10.1520/D3173.
(94) ASTM. ASTM D3175-Standard Test Method for Volatile Matter in the Analysis Sample of Coal and Coke. *ASTM Int.* **2011**, 6. https://doi.org/10.1520/D3175-11.2.
(95) ASTM. ASTM D3174: Standard Test Method for Ash in the Analysis Sample

of Coal and Coke from Coal. *ASTM Int.* **2002**, *05* (Reapproved 2018), 1–6. https://doi.org/10.1520/D3174-12R18.2.
(96) States, U. Standard Practice for Preparation of Biomass for Compositional Analysis 1. *Annu. B. ASTM Stand.* **2011**, *01* (Reapproved 2007), 6–9. https://doi.org/10.1520/E1757-01R07.2.
(97) Peng, J. H.; Bi, H. T.; Sokhansanj, S.; Lim, J. C. A Study of Particle Size Effect on Biomass Torrefaction and Densification. *Energy and Fuels* **2012**, *26* (6), 3826–3839. https://doi.org/10.1021/ef3004027.
(98) ASTM. ASTM D3176-15 Standard Practice for Ultimate Analysis of Coal and Coke. *Annu. B. ASTM Stand.* **2015**, No. 60, American Society for Testing and Materials, West C. https://doi.org/10.1520/D3176-15.2.
(99) Clarke, S.; Preto, F. *Biomass Burn Characteristics*; 2011.
(100) Braza, C. E. M.; Crnkovic, P. M. Physical - Chemical Characterization of Biomass Samples for Application in Pyrolysis Process. *Chem. Eng. Trans.* **2014**, *37*, 523–528. https://doi.org/10.3303/CET1437088.
(101) He, Y.; Yao, T.; Tan, S.; Yu, B.; Liu, K.; Hu, L.; Luo, K.; Liu, M.; Liu, X.; Bai, L. Ecotoxicology and Environmental Safety Effects of PH and Gallic Acid on the Adsorption of Two Ionizable Organic Contaminants to Rice Straw-Derived Biochar-Amended Soils. *Ecotoxicol. Environ. Saf.* **2019**, *184* (September), 109656. https://doi.org/10.1016/j.ecoenv.2019.109656.
(102) Ni, B. J.; Huang, Q. S.; Wang, C.; Ni, T. Y.; Sun, J.; Wei, W. Competitive Adsorption of Heavy Metals in Aqueous Solution onto Biochar Derived from Anaerobically Digested Sludge. *Chemosphere* **2019**, *219*, 351–357. https://doi.org/10.1016/j.chemosphere.2018.12.053.
(103) Xiao, Z.; Rasmann, S.; Yue, L.; Lian, F.; Zou, H.; Wang, Z. The Effect of Biochar Amendment on N-Cycling Genes in Soils: A Meta-Analysis. *Sci. Total Environ.* **2019**, *696*, 133984. https://doi.org/10.1016/j.scitotenv.2019.133984.
(104) IBI. *Standardized Product Definition and Product Testing Guidelines for Biochar That Is Used in Soil*; 2015. https://doi.org/http://www.biochar-international.org/characterizationstandard. 22.
(105) Sigmund, G.; Hüffer, T.; Hofmann, T.; Kah, M. Biochar Total Surface Area and Total Pore Volume Determined by N2 and CO2 Physisorption Are Strongly Influenced by Degassing Temperature. *Sci. Total Environ.* **2017**, *580*, 770–775. https://doi.org/10.1016/j.scitotenv.2016.12.023.
(106) ASTM International. Standard Test Method for Carbon Black - Total and External Surface Area by Nitrogen Adsorption. Designation: D6556 – 10 Standard. *ASTM Int.* **2012**, *i*, 1–5. https://doi.org/10.1520/D6556-10.2.
(107) Dollimore, D.; Spooner, P.; Turner, A. The BET Method of Analysis of Gas Adsorption Data and Its Relevance to the Calculation of Surface Areas. *Surf. Technol.* **1976**, *4* (2), 121–160. https://doi.org/10.1016/0376-4583(76)90024-8.
(108) Purakayastha, T. J.; Bera, T.; Bhaduri, D.; Sarkar, B.; Mandal, S.; Wade, P.; Kumari, S.; Biswas, S.; Menon, M.; Pathak, H.; et al. A Review on Biochar Modulated Soil Condition Improvements and Nutrient Dynamics Concerning Crop Yields: Pathways to Climate Change Mitigation and Global Food Security. *Chemosphere* **2019**, *227*, 345–365.

https://doi.org/10.1016/j.chemosphere.2019.03.170.
(109) Tangahu, B. V.; Sheikh Abdullah, S. R.; Basri, H.; Idris, M.; Anuar, N.; Mukhlisin, M. A Review on Heavy Metals (As, Pb, and Hg) Uptake by Plants through Phytoremediation. *Int. J. Chem. Eng.* **2011**, *2011*. https://doi.org/10.1155/2011/939161.
(110) Mehlich, A. Mehlich 3 Soil Test Extractant : A Modification of Mehlich 2 Extractant. *Commun. Soil Sci. Plant Anal.* **1984**, *15* (12), 1409–1416. https://doi.org/10.1167/iovs.11-7364.
(111) Liu, Y.; Yao, S.; Wang, Y.; Lu, H.; Brar, S. K.; Yang, S. Bio- and Hydrochars from Rice Straw and Pig Manure: Inter-Comparison. *Bioresour. Technol.* **2017**, *235* (March), 332–337. https://doi.org/10.1016/j.biortech.2017.03.103.
(112) Medic, D.; Darr, M.; Shah, A.; Rahn, S. The Effects of Particle Size, Different Corn Stover Components, and Gas Residence Time on Torrefaction of Corn Stover. *Energies* **2012**, *5* (4), 1199–1214. https://doi.org/10.3390/en5041199.
(113) Xu, Y.; Chen, B. Investigation of Thermodynamic Parameters in the Pyrolysis Conversion of Biomass and Manure to Biochars Using Thermogravimetric Analysis. *Bioresour. Technol.* **2013**, *146*, 485–493. https://doi.org/10.1016/j.biortech.2013.07.086.
(114) Ibn Ferjani, A.; Jeguirim, M.; Jellali, S.; Limousy, L.; Courson, C.; Akrout, H.; Thevenin, N.; Ruidavets, L.; Muller, A.; Bennici, S. The Use of Exhausted Grape Marc to Produce Biofuels and Biofertilizers: Effect of Pyrolysis Temperatures on Biochars Properties. *Renew. Sustain. Energy Rev.* **2019**, *107* (December 2018), 425–433. https://doi.org/10.1016/j.rser.2019.03.034.
(115) Smith, A. M.; Ross, A. B. The Influence of Residence Time during Hydrothermal Carbonisation of Miscanthus on Bio-Coal Combustion Chemistry. *Energies* **2019**, *12* (3), 13–22. https://doi.org/10.3390/en12030523.
(116) Tomczyk, A.; Sokołowska, Z.; Boguta, P. Biochar Physicochemical Properties: Pyrolysis Temperature and Feedstock Kind Effects. *Rev. Environ. Sci. Biotechnol.* **2020**, *19* (1), 191–215. https://doi.org/10.1007/s11157-020-09523-3.
(117) USDA. *Soil Quality Indicators: EC*; 2011.
(118) USDA. *Soil Quality Indicators: PH*; 1998. https://doi.org/10.2136/sssaspecpub49.c25.
(119) Volpe, M.; Goldfarb, J. L.; Fiori, L. Hydrothermal Carbonization of Opuntia Ficus-Indica Cladodes: Role of Process Parameters on Hydrochar Properties. *Bioresour. Technol.* **2018**, *247* (June 2017), 310–318. https://doi.org/10.1016/j.biortech.2017.09.072.
(120) Chowdhury, Z. Z.; Ziaul Karim, M.; Ashraf, M. A.; Khalid, K. Influence of Carbonization Temperature on Physicochemical Properties of Biochar Derived from Slow Pyrolysis of Durian Wood (Durio Zibethinus) Sawdust. *BioResources* **2016**, *11* (2), 3356–3372. https://doi.org/10.15376/biores.11.2.3356-3372.
(121) Yue, Y.; Lin, Q.; Xu, Y.; Li, G.; Zhao, X. Slow Pyrolysis as a Measure for Rapidly Treating Cow Manure and the Biochar Characteristics. *J. Anal. Appl. Pyrolysis* **2017**, *124* (January 2018), 355–361.

https://doi.org/10.1016/j.jaap.2017.01.008.
(122) Tsai, W. T.; Liu, S. C.; Chen, H. R.; Chang, Y. M.; Tsai, Y. L. Textural and Chemical Properties of Swine-Manure-Derived Biochar Pertinent to Its Potential Use as a Soil Amendment. *Chemosphere* **2012**, *89* (2), 198–203. https://doi.org/10.1016/j.chemosphere.2012.05.085.
(123) Tag, A. T.; Duman, G.; Ucar, S.; Yanik, J. Influence of Carbonization Temperature on Physicochemical Properties of Biochar Derived from Slow Pyrolysis of Durian Wood (Durio Zibethinus) Sawdust. *J. Anal. Appl. Pyrolysis* **2016**, *120*, 200–206. https://doi.org/10.1016/j.jaap.2016.05.006.
(124) Batista, E. M. C. C.; Shultz, J.; Matos, T. T. S.; Fornari, M. R.; Ferreira, T. M.; Szpoganicz, B.; De Freitas, R. A.; Mangrich, A. S. Effect of Surface and Porosity of Biochar on Water Holding Capacity Aiming Indirectly at Preservation of the Amazon Biome. *Sci. Rep.* **2018**, *8* (1), 1–9. https://doi.org/10.1038/s41598-018-28794-z.
(125) Sharma, R. K.; Wooten, J. B.; Baliga, V. L.; Lin, X.; Chan, W. G.; Hajaligol, M. R. Characterization of Chars from Pyrolysis of Lignin. *Fuel* **2004**, *83* (11–12), 1469–1482. https://doi.org/10.1016/j.fuel.2003.11.015.
(126) Li, Z.; Zhao, B.; Wang, Q.; Cao, X.; Zhang, J. Differences in Chemical Composition of Soil Organic Carbon Resulting from Long-Term Fertilization Strategies. *PLoS One* **2015**, *10* (4), 1–14. https://doi.org/10.1371/journal.pone.0124359.
(127) Pastorova, I.; Botto, R. E.; Arisz, P. W.; Boon, J. J. Cellulose Char Structure: A Combined Analytical Py-GC-MS, FTIR, and NMR Study. *Carbohydr. Res.* **1994**, *262* (1), 27–47. https://doi.org/10.1016/0008-6215(94)84003-2.
(128) Ong, H. C.; Chen, W. H.; Singh, Y.; Gan, Y. Y.; Chen, C. Y.; Show, P. L. A State-of-the-Art Review on Thermochemical Conversion of Biomass for Biofuel Production: A TG-FTIR Approach. *Energy Convers. Manag.* **2020**, *209* (December 2019), 112634. https://doi.org/10.1016/j.enconman.2020.112634.
(129) Cheng, H.; Liu, Q.; Huang, M.; Zhang, S.; Frost, R. L. Application of TG-FTIR to Study SO2 Evolved during the Thermal Decomposition of Coal-Derived Pyrite. *Thermochim. Acta* **2013**, *555*, 1–6. https://doi.org/10.1016/j.tca.2012.12.025.
(130) Coates, J. Interpretation of Infrared Spectra, A Practical Approach. In *Encyclopedia of Analytical Chemistry: Applications, Theory and Instrumentation*; 2006; pp 1–23.
(131) Liu, J.; Li, R.; Guo, M.; Tao, H.; Sun, D.; Zong, C.; Liu, C.; Fu, F. Study of the Thermal Degradation of Benzene-Containing Glycerol Carbonate Derivatives by a Combined TG–FTIR and Theoretical Calculation. *Thermochim. Acta* **2017**, *654* (February), 179–185. https://doi.org/10.1016/j.tca.2017.05.021.
(132) Odeh, A. O. Qualitative and Quantitative ATR-FTIR Analysis and Its Application to Coal Char of Different Ranks. *Ranliao Huaxue Xuebao/Journal Fuel Chem. Technol.* **2015**, *43* (2), 129–137. https://doi.org/10.1016/s1872-5813(15)30001-3.
(133) Peng, X.; Ma, X.; Lin, Y.; Guo, Z.; Hu, S.; Ning, X.; Cao, Y.; Zhang, Y. Co-Pyrolysis between Microalgae and Textile Dyeing Sludge by TG-FTIR:

Kinetics and Products. *Energy Convers. Manag.* **2015**, *100*, 391–402. https://doi.org/10.1016/j.enconman.2015.05.025.
(134) Cooke, N. E.; Fuller, O. M.; Gaikwad, R. P. FT-i.r. Spectroscopic Analysis of Coals and Coal Extracts. *Fuel* **1986**, *65* (9), 1254–1260. https://doi.org/10.1016/0016-2361(86)90238-3.
(135) Khiari, B.; Jeguirim, M. Pyrolysis of Grape Marc from Tunisian Wine Industry: Feedstock Characterization, Thermal Degradation and Kinetic Analysis. *Energies* **2018**, *11* (4). https://doi.org/10.3390/en11040730.
(136) Tan, Z.; Yuan, S.; Hong, M.; Zhang, L.; Huang, Q. Mechanism of Negative Surface Charge Formation on Biochar and Its Effect on the Fixation of Soil Cd. *J. Hazard. Mater.* **2020**, *384* (February 2019). https://doi.org/10.1016/j.jhazmat.2019.121370.
(137) Dieguez-Alonso, A.; Funke, A.; Anca-Couce, A.; Rombolà, A. G.; Ojeda, G.; Bachmann, J.; Behrendt, F. Towards Biochar and Hydrochar Engineering-Influence of Process Conditions on Surface Physical and Chemical Properties, Thermal Stability, Nutrient Availability, Toxicity and Wettability. *Energies* **2018**, *11* (3). https://doi.org/10.3390/en11030496.
(138) Fei, Y. heng; Zhao, D.; Liu, Y.; Zhang, W.; Tang, Y. yuan; Huang, X.; Wu, Q.; Wang, Y. xing; Xiao, T.; Liu, C. Feasibility of Sewage Sludge Derived Hydrochars for Agricultural Application: Nutrients (N, P, K) and Potentially Toxic Elements (Zn, Cu, Pb, Ni, Cd). *Chemosphere* **2019**, *236*, 124841. https://doi.org/10.1016/j.chemosphere.2019.124841.
(139) Parthasarathy, P.; Narayanan, S. K. Effect of Hydrothermal Carbonization Reaction Parameters On. *Environ. Prog. Sustain. Energy* **2014**, *33* (3), 676–680. https://doi.org/10.1002/ep.
(140) Xiao, X.; Chen, B.; Chen, Z.; Zhu, L.; Schnoor, J. L. Insight into Multiple and Multilevel Structures of Biochars and Their Potential Environmental Applications: A Critical Review. *Environ. Sci. Technol.* **2018**, *52* (9), 5027–5047. https://doi.org/10.1021/acs.est.7b06487.
(141) Wang, F.; Zhang, D.; Chen, M.; Yi, W.; Wang, L. Characteristics of Corn Stover Components Pyrolysis at Low Temperature Based on Detergent Fibers. *Front. Bioeng. Biotechnol.* **2019**, *7* (AUG), 1–9. https://doi.org/10.3389/fbioe.2019.00188.
(142) Tartarelli, R.; Giorgini, M.; Ghetti, P.; Belli, R. DTG Combustion Behaviour of Charcoals. *Fuel* **1987**, *66* (12), 1737–1738. https://doi.org/10.1016/0016-2361(87)90373-5.
(143) Demirbaş, A.; Demirbaş, A. H. Estimating the Calorific Values of Lignocellulosic Fuels. *Energy Explor. Exploit.* **2004**, *22* (2), 135–143. https://doi.org/10.1260/0144598041475198.
(144) Rafiq, M. K.; Bachmann, R. T.; Rafiq, M. T.; Shang, Z.; Joseph, S.; Long, R. L. Influence of Pyrolysis Temperature on Physico-Chemical Properties of Corn Stover (Zea Mays l.) Biochar and Feasibility for Carbon Capture and Energy Balance. *PLoS One* **2016**, *11* (6), 1–17. https://doi.org/10.1371/journal.pone.0156894.
(145) Font-Palma, C. Methods for the Treatment of Cattle Manure—A Review. *J.*

carbon Res. **2019**, *5* (27). https://doi.org/10.3390/c5020027.
(146) Chen, D.; Zhou, J.; Zhang, Q.; Zhu, X. Evaluation Methods and Research Progresses in Bio-Oil Storage Stability. *Renew. Sustain. Energy Rev.* **2014**, *40*, 69–79. https://doi.org/10.1016/j.rser.2014.07.159.
(147) Naik, C. V.; Westbrook, C. K.; Herbinet, O.; Pitz, W. J.; Mehl, M. Detailed Chemical Kinetic Reaction Mechanism for Biodiesel Components Methyl Stearate and Methyl Oleate. *Proc. Combust. Inst.* **2011**, *33* (1), 383–389. https://doi.org/10.1016/j.proci.2010.05.007.
(148) Jacobson, K.; Maheria, K. C.; Kumar Dalai, A. Bio-Oil Valorization: A Review. *Renew. Sustain. Energy Rev.* **2013**, *23*, 91–106. https://doi.org/10.1016/j.rser.2013.02.036.
(149) Oasmaa, A.; Elliott, D. C.; Korhonen, J. Acidity of Biomass Fast Pyrolysis Bio-Oils. *Energy and Fuels* **2010**, *24* (12), 6548–6554. https://doi.org/10.1021/ef100935r.

APPENDIX

A. Figures. This appendix includes the remaining mixtures of the DTG curves from the initial biomasses, hydrochars, and biochars

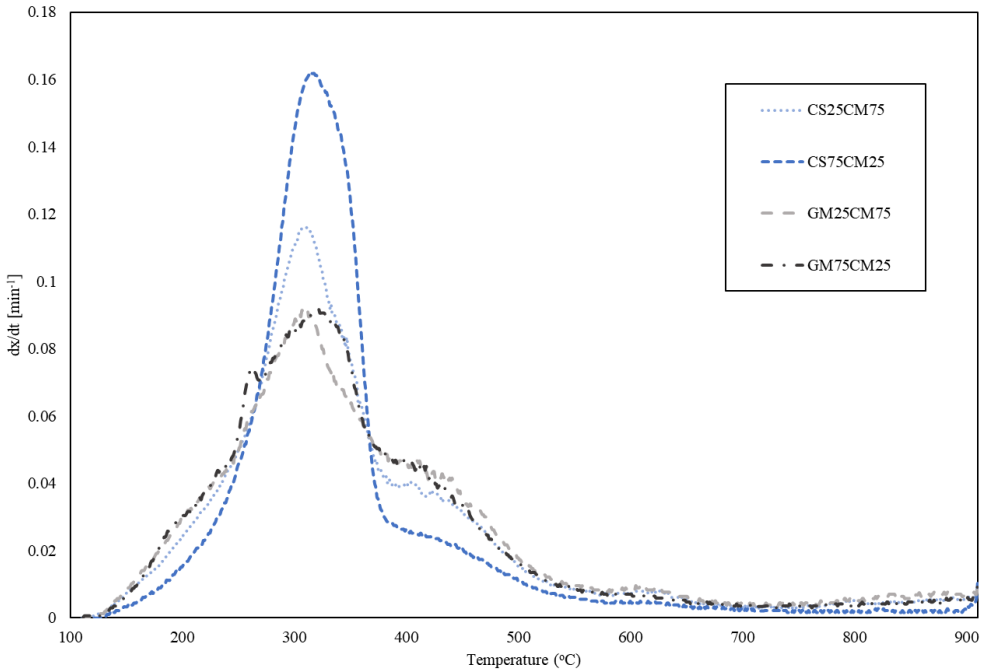

Figure 15. DTG curves of the initial biomasses remaining mixtures

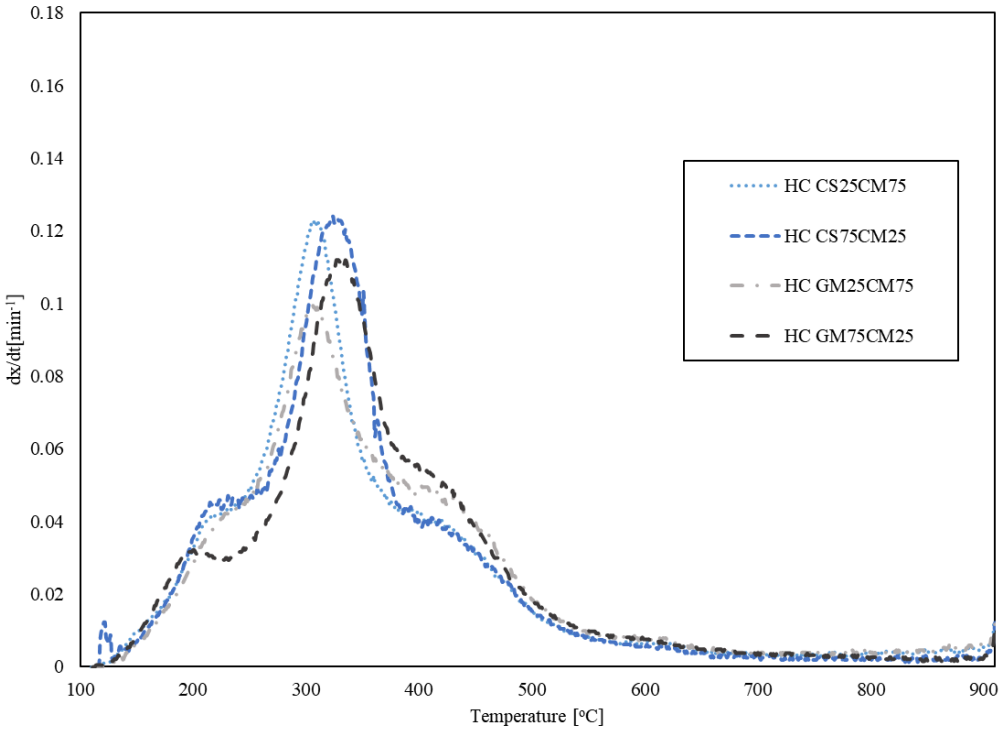

Figure 16. DTG curves of the hydrochars remaining mixtures

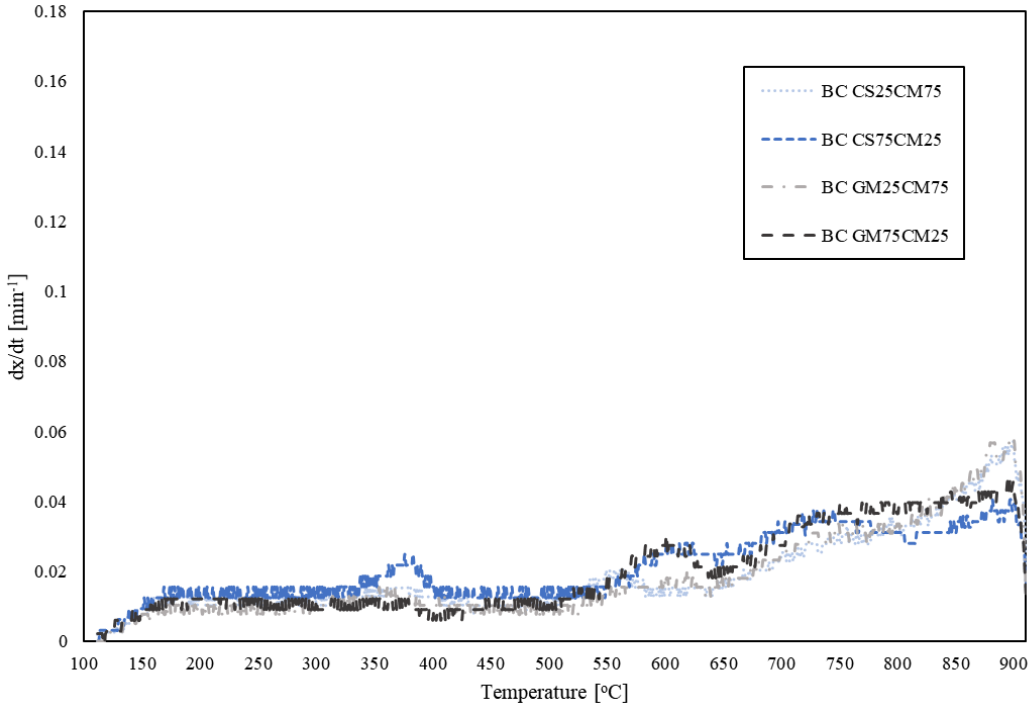

Figure 17. DTG curves of the biochars remaining mixtures

B. Tables. This appendix includes detailed organic compounds found in the bio-oil produced during pyrolysis

Table 15. Organics in bio-oil from pyrolysis - Ketones and derivatives

#	t	Products		CS	2hr HC CM	GM	CS25CM75	CS50CM50	CS75CM25	GM25CM75	GM50CM50	GM75CM25
		Ketones and derivatives										
1	7.2	2-Cyclopenten-1-one	Area	7.73E+05	2.15E+05	6.80E+05	1.28E+06	1.02E+06	1.29E+06	7.68E+05	7.58E+05	1.08E+06
	7.2		Area %	6.46	1.67	2.00	3.80	6.24	6.91	1.88	2.42	2.81
2	11.3	2-Cyclopenten-1-one, 2-methyl-	Area	3.49E+05	1.43E+05	5.68E+05	6.26E+05	4.32E+05	5.89E+05	7.76E+05	4.51E+05	7.20E+05
	11.3		Area %	2.91	1.12	1.67	1.87	2.65	3.16	1.90	1.44	1.88
3	15.4	2-Cyclopenten-1-one, 3-methyl-	Area	3.93E+05	-	-	5.57E+05	4.26E+05	5.54E+05	-	3.94E+05	-
	15.4		Area %	3.28	-	-	1.66	2.62	2.97	-	1.25	-
4	18.0	2-Cyclopenten-1-one, 2,3-dimethyl-	Area	3.08E+05	-	4.04E+05	5.35E+05	4.58E+05	5.50E+05	4.69E+05	2.89E+05	4.69E+05
	21.1		Area %	2.57	-	1.19	1.60	2.82	2.94	1.15	0.92	1.22
5	20.2	yclopenten-1-one, 2-hydroxy-3-met	Area	3.76E+05	-	-	5.72E+05	4.78E+05	5.48E+05	-	-	-
	20.2		Area %	3.14	-	-	1.71	2.94	2.94	-	-	-
6	26.4	2-Cyclohexen-1-one, 4,4-dimethyl-	Area	1.07E+05	-	-	-	-	-	-	-	-
	26.4		Area %	0.89	-	-	-	-	-	-	-	-
7	27.8	yclopenten-1-one, 3-ethyl-2-hydro	Area	1.42E+05	-	-	3.27E+05	2.26E+05	2.26E+05	-	-	-
	27.8		Area %	1.19	-	-	0.98	1.39	1.21	-	-	-
8	8.6	2-Butanone	Area	1.49E+05	-	-	-	-	-	-	-	-
	8.6		Area %	1.24	-	-	-	-	-	-	-	-
9	11.6	Butyrolactone	Area	7.69E+05	3.19E+05	1.37E+06	1.14E+06	1.00E+06	1.19E+06	9.86E+05	1.11E+06	1.74E+06
	11.7		Area %	6.43	2.49	4.05	3.41	6.15	6.40	2.41	3.54	4.54
10	9.3	2-Propanone, 1-(acetyloxy)-	Area	6.17E+05	-	3.02E+05	-	3.74E+05	6.22E+05	-	-	3.97E+05
	9.3		Area %	5.16	-	0.89	-	2.30	3.33	-	-	1.04
11	11.5	2(5H)-Furanone	Area	2.19E+05	-	-	-	-	1.65E+05	-	-	-
	11.6		Area %	1.83	-	-	-	-	0.89	-	-	-
12	12.6	1,2-Cyclopentanedione	Area	2.25E+05	-	-	-	-	1.41E+05	-	-	-
	12.6		Area %	1.88	-	-	-	-	0.76	-	-	-
13	13.6	Bicyclo[3.2.0]heptan-2-one	Area	6.42E+04	-	-	-	-	-	-	-	-
	13.6		Area %	0.54	-	-	-	-	-	-	-	-
14	16.0	2-Butanone, 1-(acetyloxy)-	Area	1.06E+05	-	-	-	-	1.14E+05	-	-	-
	16.0		Area %	0.88	-	-	-	-	0.61	-	-	-
15	16.2	2(5H)-Furanone, 3-methyl-	Area	6.56E+04	-	-	-	-	-	-	-	-
	16.2		Area %	0.55	-	-	-	-	-	-	-	-
16	17.7	4,4-Dimethyl-2-cyclopenten-1-one	Area	5.32E+04	-	-	-	-	-	-	-	-
	17.7		Area %	0.44	-	-	-	-	-	-	-	-
17	18.2	-Furanone, 2,5-dihydro-3,5-dimethy	Area	8.33E+04	-	-	-	-	9.51E+04	-	-	-
	18.2		Area %	0.70	-	-	-	-	0.51	-	-	-
18	10.6	2-Heptanone	Area	-	-	2.77E+05	-	-	-	-	-	-
	10.6		Area %	-	-	0.82	-	-	-	-	-	-
19	25.9	2,5-Pyrrolidinedione, 1-methyl-	Area	-	-	2.86E+05	-	-	-	-	-	-
	25.9		Area %	-	-	0.84	-	-	-	-	-	-
20	15.8	3-Pentanone, 2-methyl-	Area	-	-	-	-	-	1.21E+05	-	-	-
	15.8		Area %	-	-	-	-	-	0.65	-	-	-
21	15.3	bicyclo[3.3.0]oct-7-en-2-one, 7-met	Area	-	-	-	-	-	-	-	-	9.53E+05
	15.3		Area %	-	-	-	-	-	-	-	-	2.49

Table 16. Organics in bio-oil from pyrolysis - Phenols and derivatives

#	t	Products		CS	2hr HC CM	GM	CS25CM75	CS50CM50	CS75CM25	GM25CM75	GM50CM50	GM75CM25
		Phenols and derivatives										
22	17.1	Phenol	Area	8.81E+05	1.04E+06	3.07E+06	2.63E+06	1.27E+06	1.63E+06	2.76E+06	2.85E+06	2.85E+06
	17.2		Area %	7.36	8.09	9.03	7.84	7.78	8.76	6.75	9.07	7.45
23	23.0	Phenol, 2-methyl-	Area	1.88E+05	5.54E+05	1.09E+06	6.43E+05	2.93E+05	1.03E+06	7.31E+05	8.68E+05	1.98E+06
	24.9		Area %	1.57	4.32	3.22	1.92	1.80	5.55	1.79	2.77	5.17
24	25.0	Phenol, 3-methyl-	Area	-	-	2.53E+06	-	-	-	-	2.06E+06	-
	24.9		Area %	-	-	7.46	-	-	-	-	6.55	-
25	23.2	Phenol, 2-methoxy-	Area	6.50E+05	1.02E+06	4.70E+06	2.71E+06	1.51E+06	1.45E+06	3.11E+06	3.05E+06	5.50E+06
	25.4		Area %	5.43	7.92	13.84	8.09	9.25	7.78	7.60	9.71	14.37
26	30.8	Phenol, 3,4-dimethyl-	Area	5.02E+04	-	-	-	-	-	-	-	-
	30.8		Area %	0.42	-	-	-	-	-	-	-	-
27	32.4	Phenol, 4-ethyl-	Area	2.19E+05	2.20E+05	3.42E+05	9.49E+05	3.55E+05	4.54E+05	7.27E+05	4.92E+05	4.91E+05
	32.4		Area %	1.83	1.72	1.01	2.83	2.19	2.44	1.78	1.57	1.28
28	40.9	Phenol, 4-ethyl-2-methoxy-	Area	1.70E+05	2.90E+05	2.12E+06	1.07E+06	4.63E+05	4.38E+05	1.05E+06	1.28E+06	1.99E+06
	41.0		Area %	1.42	2.26	6.26	3.19	2.85	2.35	2.57	4.08	5.20
29	46.7	Phenol, 2,6-dimethoxy-	Area	2.66E+05	4.23E+05	-	1.27E+06	5.22E+05	6.18E+05	9.24E+05	6.54E+05	5.08E+05
	46.7		Area %	2.23	3.30	-	3.78	3.21	3.31	2.26	2.08	1.33
30	24.8	p-Cresol	Area	4.48E+05	3.11E+05	-	1.56E+06	6.42E+05	4.34E+05	1.72E+06	-	1.35E+06
	24.9		Area %	3.74	2.43	-	4.65	3.94	2.33	4.21	-	3.53
31	34.0	Creosol	Area	5.31E+04	-	1.98E+06	4.34E+05	1.66E+05	1.86E+05	7.28E+05	1.03E+06	1.90E+06
	34.0		Area %	0.44	-	5.85	1.29	1.02	1.00	1.78	3.29	4.97
32	43.8	2-Methoxy-4-vinylphenol	Area	4.48E+05	-	3.13E+05	-	3.24E+05	5.26E+05	-	-	-
	43.8		Area %	3.74	-	0.92	-	1.99	2.82	-	-	-
33	30.8	Phenol, 2,4-dimethyl-	Area	-	-	4.52E+05	-	-	-	-	3.02E+05	4.23E+05
	30.9		Area %	-	-	1.33	-	-	-	-	0.96	1.10
34	31.0	Phenol, 2,5-dimethyl-	Area	-	-	3.26E+05	-	-	-	-	-	-
	31.0		Area %	-	-	0.96	-	-	-	-	-	-
35	32.6	Phenol, 2-ethyl-	Area	-	-	2.37E+05	-	-	-	-	-	-
	32.6		Area %	-	-	0.70	-	-	-	-	-	-
36	30.8	Phenol, 3,5-dimethyl-	Area	-	-	2.46E+05	-	-	1.34E+05	-	-	-
	32.7		Area %	-	-	0.73	-	-	0.72	-	-	-
37	47.9	Phenol, 2-methoxy-4-propyl	Area	-	-	4.96E+05	-	-	-	-	6.70E+05	-
	47.9		Area %	-	-	1.46	-	-	-	-	1.89	-
38	54.2	trans-Isoeugenol	Area	-	-	5.77E+05	-	-	-	-	2.47E+05	5.44E+05
	54.3		Area %	-	-	1.70	-	-	-	-	0.79	1.42
39	31.0	Phenol, 2,6-dimethyl-	Area	-	-	-	-	1.63E+05	-	-	-	-
	31.0		Area %	-	-	-	-	0.88	-	-	-	-
40	25.4	Phenol, 2-methoxy-	Area	-	-	-	-	-	1.34E+06	-	-	-
	25.4		Area %	-	-	-	-	-	7.18	-	-	-

Table 17. Organics in bio-oil from pyrolysis - Alkanes and derivatives

#	t	Products		CS	2hr HC CM	GM	CS25CM75	CS50CM50	CS75CM25	GM25CM75	GM50CM50	GM75CM25
		Alkanes and derivatives										
41	58.7	Heneicosane	Area	1.61E+05	1.35E+06	3.21E+06	7.42E+05	2.80E+05	2.37E+06	2.49E+06	9.66E+05	2.08E+06
	94.0		Area %	1.26	10.56	9.52	2.21	1.72	5.78	6.56	3.08	5.42
42	35.5	Dodecane	Area	-	1.84E+05	2.66E+05	3.89E+05	-	-	8.34E+05	3.61E+05	3.56E+05
	35.5		Area %	-	1.43	0.78	1.16	-	-	2.04	1.15	0.93
43	43.6	Tetradecane	Area	-	5.96E+05	9.79E+05	1.41E+06	1.42E+05	-	1.29E+06	7.37E+05	1.15E+06
	51.4		Area %	-	4.65	2.88	4.64	0.87	-	3.14	2.35	2.99
44	58.6	Heptadecane	Area	-	1.56E+06	-	1.19E+06	-	-	1.64E+06	1.08E+06	8.85E+05
	58.7		Area %	-	6.84	-	4.17	-	-	4	3.43	2.31
45	94.0	Eicosane	Area	-	7.44E+05	3.84E+05	1.67E+06	2.89E+05	1.71E+05	2.85E+06	1.33E+06	5.85E+05
	105.3		Area %	-	5.8	1.13	5	1.78	0.92	6.97	4.24	1.53
46	27.1	Undecane	Area	-	-	2.39E+05	-	-	-	6.78E+05	-	-
	27.2		Area %	-	-	0.7	-	-	-	1.66	-	-
47	110.4	Hexatriacontane	Area	-	2.15E+05	-	-	1.44E+05	-	6.24E+05	-	-
	110.4		Area %	-	1.67	-	-	0.89	-	1.52	-	-
48	110.4	Dotriacontane	Area	-	1.98E+05	-	8.19E+05	-	-	1.39E+06	9.56E+05	-
	120.0		Area %	-	1.54	-	2.44	-	-	3.4	3.05	-
49	110.4	Tetracontane	Area	-	-	-	4.74E+05	-	-	-	-	-
	110.4		Area %	-	-	-	1.41	-	-	-	-	-
50	26.4	Bicyclo[3.3.1]nonane	Area	-	-	-	-	1.40E+05	2.04E+05	-	-	-
	26.4		Area %	-	-	-	-	0.86	1.1	-	-	-
51	99.9	2-Methylhexacosane	Area	-	-	-	-	3.74E+05	-	-	-	-
	99.9		Area %	-	-	-	-	2.3	-	-	-	-
52	43.6	Pentadecane	Area	-	-	-	-	-	-	1.02E+06	5.23E+05	-
	43.6		Area %	-	-	-	-	-	-	2.5	1.67	-
53	26.3	Cyclododecane	Area	-	-	-	-	-	-	-	-	3.44E+05
	26.3		Area %	-	-	-	-	-	-	-	-	0.9

Table 18. Organics in bio-oil from pyrolysis - Alkenes and derivatives

#	t	Products		CS	2hr HC CM	GM	CS25CM75	CS50CM50	CS75CM25	GM25CM75	GM50CM50	GM75CM25
		Alkenes and derivatives										
54	34.8	1-Dodecene	Area	-	1.13E+05	-	-	-	-	-	-	-
	34.8		Area %	-	0.88	-	-	-	-	-	-	-
55	42.9	1-Pentadecene	Area	-	1.55E+05	-	2.95E+05	-	-	4.78E+05	7.85E+05	-
	50.7		Area %	-	1.21	-	0.88	-	-	1.17	2.27	-
56	58.0	1-Heptadecene	Area	-	7.05E+05	-	3.58E+05	-	-	1.52E+06	3.90E+05	3.93E+05
	72.2		Area %	-	4.3	-	1.07	-	-	3.72	1.24	1.03
57	26.4	1-Undecene	Area	-	-	-	-	-	-	4.75E+05	-	-
	26.4		Area %	-	-	-	-	-	-	1.16	-	-
58	50.7	1-Tetradecene	Area	-	-	-	-	-	-	7.49E+05	-	-
	50.7		Area %	-	-	-	-	-	-	1.83	-	-
59	65.0	1-Nonadecene	Area	-	-	-	-	-	-	7.99E+05	-	-
	72.2		Area %	-	-	-	-	-	-	2.18	-	-

Table 19. Organics in bio-oil from pyrolysis - Acids and derivatives

#	t	Products		CS	2hr HC CM	GM	CS25CM75	CS50CM50	CS75CM25	GM25CM75	GM50CM50	GM75CM25
		Acids and derivatives										
60	18.8	Butanoic acid, anhydride	Area	-	1.40E+05	-	-	-	-	-	-	-
	18.8		Area %	-	1.09	-	-	-	-	-	-	-
61	33.0	Benzeneacetic acid, methyl ester	Area	-	2.28E+05	-	4.52E+05	-	-	-	-	-
	33.0		Area %	-	1.78	-	1.35	-	-	-	-	-
62	75.0	etic acid, 3,7,11,15-tetramethyl-hexadecyl es	Area	-	1.11E+05	-	3.76E+05	2.44E+05	3.29E+05	-	-	-
	75.1		Area %	-	0.87	-	1.12	1.5	1.76	-	-	-
63	80.2	Heneicosanoic acid, methyl ester	Area	-	1.23E+05	-	-	-	-	-	-	-
	80.2		Area %	-	0.95	-	-	-	-	-	-	-
64	89.2	Hexadecanoic acid, methyl ester	Area	-	6.37E+05	7.15E+05	1.40E+06	3.53E+05	1.94E+05	1.73E+06	1.74E+06	1.32E+06
	89.3		Area %	-	4.96	2.11	4.17	2.17	1.04	4.24	5.55	3.44
65	119.9	Nonahexacontanoic acid	Area	-	3.46E+05	-	-	-	-	-	-	-
	119.9		Area %	-	2.7	-	-	-	-	-	-	-
66	101.2	Methyl stearate	Area	-	1.30E+06	2.82E+05	3.13E+06	8.12E+05	3.37E+05	-	2.13E+06	9.53E+05
	101.2		Area %	-	10.11	0.83	9.33	4.99	1.81	-	6.79	2.49
67	8.0	Butanoic acid, 3-methyl-	Area	-	-	-	-	-	1.29E+05	-	-	-
	8.0		Area %	-	-	-	-	-	0.69	-	-	-
68	18.8	Propanoic acid, 2-methyl-, anhydride	Area	-	-	-	-	-	-	-	2.54E+05	-
	18.8		Area %	-	-	-	-	-	-	-	0.81	-
69	99.5	9-Octadecenoic acid, methyl ester, (E)-	Area	-	-	-	-	1.75E+05	-	6.60E+05	7.30E+05	6.98E+05
	99.5		Area %	-	-	-	-	1.08	-	1.61	2.32	1.82

Table 20. Organics in bio-oil from pyrolysis - Aldehydes and derivatives

#	t	Products		CS	2hr HC CM	GM	CS25CM75	CS50CM50	CS75CM25	GM25CM75	GM50CM50	GM75CM25
		Aldehydes, Alcohols and derivatives										
70	6.5	3-Furaldehyde	Area	1.18E+06	-	2.23E+06	-	5.29E+05	1.02E+06	-	7.28E+05	2.10E+06
	7.3		Area %	9.85	-	6.58	-	3.25	5.45	-	2.32	5.49
71	15.4	2-Furancarboxaldehyde, 5-methyl-	Area	-	-	9.65E+05	-	-	-	-	-	-
	15.4		Area %	-	-	2.84	-	-	-	-	-	-
72	8.4	3-Furanmethanol	Area	6.88E+05	-	-	-	5.82E+05	8.05E+05	-	-	-
	8.5		Area %	5.75	-	-	-	3.58	4.32	-	-	-
73	15.7	1,2-Ethanediol, dipropanoate	Area	1.03E+05	-	-	-	-	-	-	-	-
	15.7		Area %	0.86	-	-	-	-	-	-	-	-
74	18.8	2-Furanmethanol, tetrahydro-	Area	2.89E+05	-	-	5.79E+05	5.76E+05	5.37E+05	7.30E+05	-	5.35E+05
	18.9		Area %	2.42	-	-	1.73	3.54	2.88	1.78	-	1.4
75	25.7	Cyclopropyl carbinol	Area	5.63E+05	-	-	-	4.09E+05	6.94E+05	-	-	-
	25.8		Area %	4.7	-	-	-	2.51	3.73	-	-	-
76	8.4	2-Furanmethanol	Area	-	-	6.55E+05	5.19E+05	-	-	-	6.11E+05	1.18E+06
	8.5		Area %	-	-	1.93	1.55	-	-	-	1.95	3.08

Table 21. Organics in bio-oil from pyrolysis - Others

#	t	Products		CS	2hr HC CM	GM	CS25CM75	CS50CM50	CS75CM25	GM25CM75	GM50CM50	GM75CM25
		Others										
77	35.8	1,4:3,6-Dianhydro-.alpha.-d-glucopyranose	Area	7.02E+04	-	-	-	-	-	-	-	-
	35.8		Area %	0.59	-	-	-	-	-	-	-	-
78	36.8	Benzofuran, 2,3-dihydro-	Area	5.94E+05	-	-	-	3.24E+05	6.68E+05	-	-	-
	36.8		Area %	4.96	-	-	-	1.99	3.59	-	-	-
79	87.2	Heptadecanenitrile	Area	1.85E+05	-	7.11E+05	-	1.39E+05	-	5.68E+05	3.13E+05	5.54E+05
	87.3		Area %	1.44	-	2.09	-	0.85	-	1.39	1	1.45
80	20.8	D-Limonene	Area	-	1.14E+05	-	-	-	-	-	-	-
	20.8		Area %	-	0.89	-	-	-	-	-	-	-
81	42.2	Indole	Area	-	1.82E+05	-	5.03E+05	1.62E+05	-	5.60E+05	4.80E+05	4.82E+05
	42.2		Area %	-	1.42	-	1.5	0.99	-	1.37	1.53	1.26
82	100.9	(Z)-18-Octadec-9-enolide	Area	-	2.96E+05	-	7.20E+05	2.84E+05	-	5.92E+05	3.57E+05	-
	101.0		Area %	-	2.31	-	2.15	1.75	-	1.45	1.14	-
83	25.8	t-Butyl 1-piperaziencarboxylate	Area	-	-	-	-	-	-	-	-	4.77E+05
	25.8		Area %	-	-	-	-	-	-	-	-	1.24
84	33.2	Naphthalene	Area	-	-	3.57E+05	-	-	-	-	-	-
	33.2		Area %	-	-	1.05	-	-	-	-	-	-